

A stabilizer code model with non-invertible symmetries: Strange fractons, confinement, and non-commutative and non-Abelian fusion rules

Tanay Kibe* and Ayan Mukhopadhyay[†]

*Center for Strings, Gravitation and Cosmology,
and Center for Operator Algebras, Geometry, Matter and Spacetime,
Indian Institute of Technology Madras, Chennai 600036, India*

Pramod Padmanabhan[‡]

School of Basic Sciences, Indian Institute of Technology, Bhubaneswar, 752050, India

We introduce a stabilizer code model with a qutrit at every edge on a square lattice and with non-invertible plaquette operators. The degeneracy of the ground state is topological as in the toric code, and it also has the usual deconfined excitations consisting of pairs of electric and magnetic charges. However, there are novel types of confined fractonic excitations composed of a cluster of adjacent faces (defects) with vanishing flux. They manifest confinement, and even larger configurations of these fractons are fully immobile although they acquire emergent internal degrees of freedom. Deconfined excitations change their nature in presence of these fractonic defects. As for instance, a magnetic monopole can exist anywhere on the lattice exterior to a fractonic defect cluster while electric charges acquire restricted mobility. These imply that our model featuring fractons is neither of type I, nor of type II. Furthermore, local operators which are symmetries can annihilate any ground state and also the full sector of states which can decay to a ground state under local perturbations. All these properties can be captured via a novel type of *non-commutative* and *non-Abelian* fusion category in which the product is associative but does not commute, and can be expressed as a sum of (operator) equivalence classes which includes that of the *zero* operator. We introduce many other variants of this model and discuss their relevance in quantum field theory.

CONTENTS

I. Introduction and Summary of Results	2
II. The model	5
A. Ground states have topological degeneracy	6

* tanayk@smail.iit.ac.in

[†] ayan@physics.iitm.ac.in

[‡] pramod23phys@gmail.com

B. Symmetries: stabilizer monoid, annihilator monoid and logical operators	7
III. The excited states	11
A. Deconfined excitations	11
B. Fractonic excitations: Confined immovable defects and their internal states	13
C. Deconfined stuff and fractons: Magnetic monopoles and restricted electric charges	19
IV. A novel fusion category: Non-commutative and non-Abelian	21
A. An intuitive discussion	21
B. Generalization of the fusion category	24
C. Fusion rules of the model	26
V. Outroduction	33
Acknowledgments	35
A. Trace computations	36
1. Isolated defect faces are disallowed	36
2. Degeneracy of two zero flux face defects	37
3. Degeneracy of three zero flux face defects	38
4. Degeneracy of four zero flux face defects	39
References	40

I. INTRODUCTION AND SUMMARY OF RESULTS

Our understanding of symmetries of physical systems has recently undergone a profound transformation [1–4]. Firstly, the notion of symmetries has been extended by studying their action not only on local operators but also on topological operators and defects. Secondly, it has been understood that such generalized symmetry operations are not necessarily invertible. Non-invertible generalized symmetries have now been found ubiquitously, as for instance, even in the standard model of particle physics after the inclusion of topological defects [5–7], and also in many condensed matter systems such as the Ising model [2, 3, 8].

In a parallel development, a new class of quasiparticles has been discovered in a variety of systems which are fully immobile or quasi-immobile (implying that they have mobility only along sub-manifolds) [9, 10]. A typical feature of such systems featuring fractonic excitations is that the

degeneracy of ground states scale with the size of the system and can also depend on the details of the lattice. These exotic fractonic quasiparticles have been partially integrated into the quantum field theory framework via symmetric tensor gauge theories [11, 12] and its variants which explains the (complete or partial) immobility of the fractons in terms of higher moment symmetries [13–21] (see also [22–29]).

A natural question, therefore is, whether one can find models with non-invertible (generalized) symmetries in which fractonic quasiparticles exist, and whether such models where non-invertible symmetries have a natural action on fractonic quasiparticles can be incorporated into quantum field theory framework. A natural place to look for such solvable models are stabilizer codes in which the Hamiltonian can be written in terms of elementary plaquette and dual plaquette operators (equivalently vertex operators), called elementary stabilizers, all of which commute with each other [30, 31]. In fact, stabilizer codes naturally feature fractons [32, 33]. Furthermore, the phases of stabilizer codes along with the quasiparticles and their fusion rules can be often incorporated into the gauge theory framework [34–41]. One can hope that stabilizer code models featuring fractons and non-invertible symmetries, can be incorporated into quantum field theory framework leading to novel quantum field theories with wide ranging applications. Particularly, we will show that a model with non-invertible symmetries and fractonic excitations necessitates the construction of novel non-commutative and non-Abelian fusion rules to characterize the excitations.¹ It will be interesting to see how such a fusion category can be incorporated into a quantum field theory.

In this work, we construct a simple and exactly solvable stabilizer code model with a qutrit (3 level system) on each edge of a two-dimensional lattice and which naturally generalizes the toric code (with a qubit on each edge) such that some of the elementary stabilizers are non-invertible. Thus the model has a strikingly intrinsic non-invertible symmetry, in the sense that it is built into the Hamiltonian of the theory itself. The full symmetries of the model are essentially of three types, (i) those which keep any ground state invariant forming the *stabilizer monoid*, (ii) logical operators which have non-trivial actions on the ground states, and (iii) those which annihilate the ground states forming the *stabilizer monoid*. In our model, the stabilizer monoid is not generated simply by the elementary stabilizers, but also by non-invertible operators supported on contractible loops of arbitrary sizes (and therefore similar to generalized symmetries). Furthermore, our model has local operators which can be supported even on a single edge, which commute with all stabilizers

¹ In this work, we will be interested not in the fusion category of only the symmetries but rather that of the superselection sectors of excitations of the theory, e.g. in the case of anyon fusion rules [30, 42]. The latter is similar to the fusion rules in conformal field theories [43] which arise as a consequence of operator product expansion of primary operators. In our construction, the symmetries which are *logical operators* close non-trivially under fusion rules, and some of these logical operators are non-invertible. However, we will avoid these logical operators for simplicity by localizing excitations on a finite subregion of the lattice.

(and therefore are symmetries) and can annihilate any ground state (and also some sectors with mobile excitations). Such symmetries have a natural action on the fractonic excitations, and in fact can detect the location of these excitations. Also some of the non-local elements of the stabilizer monoid can detect the locations of the fractonic defects and their internal states.

When restricted to the full sector of states that can decay to a ground state in the presence of local perturbations, the symmetries, which form the stabilizer monoid and the set of logical operators, act as unitary transformations (representing the action of \mathbb{Z}_2), while the annihilator monoid annihilates this entire sector of states. However, outside of this sector, even the stabilizer monoid and the logical operators are not necessarily invertible.

Interestingly, although our model has fractonic excitations, the degeneracy of the ground states is exactly like the toric code, and is therefore determined only by the genus of the lattice and not its size. In the concluding section, we will introduce a general family of such models with non-invertible symmetries in which this need not be the case (the ground state degeneracy can scale with the system size and there exists fractonic excitations). Nevertheless, it is worth mentioning that our model also has whole superselection sectors with deconfined mobile excitations that can decay to each ground state in presence of local perturbations. The fractonic excitations form new superselection sectors with finite energy barrier and therefore they are reminiscent of dark matter if the mobile excitations which can decay to the ground state are analogous to visible matter in the Universe.² These mobile excitations are exactly like those in the toric code, consisting of pairs of deconfined electric or magnetic charges (these are \mathbb{Z}_2 gauge theory charges).

The primary fractonic excitations of our model are essentially connected clusters of face excitations with vanishing fluxes and in which each face shares at least one edge with another such face. Their immobility is rather extreme in the sense that they cannot be translated by any local operation, even accounting for an arbitrary energy cost.³ Furthermore, the zero flux face can be separated from the cluster only at the cost of creating other such face excitations, implying that the energy of the cluster grows linearly with the size. The latter is the hallmark of confinement. Furthermore, larger fractonic clusters are also completely immobile, but interestingly they acquire emergent internal degrees of freedom. Our fractons are not of type I [33, 45–47], as larger configurations of fractons do not gain even partial mobility although they gain novel internal degrees of freedom.

Remarkably, the deconfined electric and magnetic charges change their nature in presence of

² This is only a provocative analogy. Here we are not claiming that we have a new theory for dark matter.

³ In this aspect, the fractons in our model are partially similar to the elementary fractons in [44]. However, in the latter model, fracton bound states are mobile.

fractonic configurations. Particularly, a magnetic monopole can exist outside a fractonic cluster although it cannot exist otherwise. This magnetic monopole is also locally mobile. However, it cannot decay to a ground state in presence of local perturbations. Since some excitations which are not localized cannot also decay to the ground state, our fracton model is not of type II category [32, 48] as well.⁴ The deconfined electric charges acquire restricted mobility in presence of fractonic defects as they cannot penetrate through them without annihilating the state (similar to the case of electrons obeying the Pauli exclusion principle).

We show that all the physical properties of the model can be characterized by novel fusion rules, which require the zero operator for closure, and which are both non-commutative and non-Abelian. The construction of the fusion rules will require us to define operator equivalence classes in a novel way. The most striking aspect of the fusion rules is that fusion products of fractonic defect superselection sectors with the identity sector can be both non-commutative and non-Abelian reflecting the fact that non-local non-invertible symmetry operators which are part of the stabilizer monoid (symmetries which leave any ground state invariant) can detect the location of fractonic defects. Furthermore, such non-trivial products are necessary for the fusion rules to be associative.

The paper is organized as follows. In Section II, we introduce the model, prove that its ground state degeneracy is determined by the genus of the lattice, and discuss the symmetries. In Section III, we discuss the deconfined excited states, the confined fractonic defects and how the deconfined fractonic excited states change their nature in the presence of fractonic defect configurations. In Section IV, we construct the fusion rules of the model, which involve the zero operator for closure, and which are both non-commutative and non-Abelian. We also discuss how the fusion rules capture the physical nature of the excitations. In Section V, we conclude by introducing more variants of our model and discussing the relevance of our work in extending the quantum field theory framework.

II. THE MODEL

A stabilizer code model is a quantum system defined on a lattice with a Hamiltonian that is a sum of local commuting operators, a.k.a. elementary stabilizers. Here we introduce such a model where each edge on a square lattice⁵ hosts a qutrit (\mathbb{C}^3) generalizing the \mathbb{Z}_2 -toric code introduced in [30] where each edge hosts a qubit (\mathbb{C}^2).

⁴ A stricter notion of type II class is that all the excitations of the system are completely immobile. Here we are employing the notion of type II class discussed in [10].

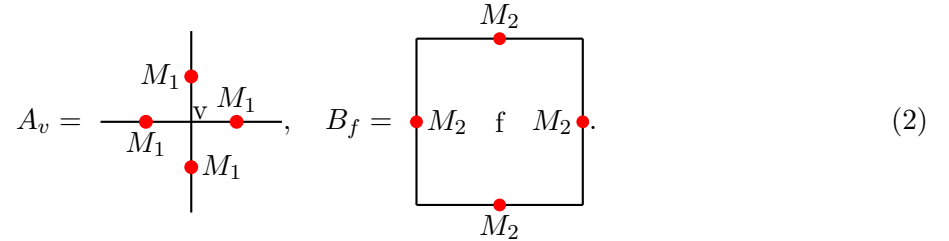
⁵ The model is well defined on an arbitrary tiling of a Riemann surface with or without boundaries. The square lattice is used for simplicity and it sufficiently describes the system's features.

Let us define the following Hermitian operators $M_{1,2}$ that act on this qutrit Hilbert space:

$$M_1 \equiv \begin{pmatrix} -1 & 0 & 0 \\ 0 & 0 & 1 \\ 0 & 1 & 0 \end{pmatrix} = (-1) \oplus X, \quad M_2 \equiv \begin{pmatrix} 0 & 0 & 0 \\ 0 & 1 & 0 \\ 0 & 0 & -1 \end{pmatrix} = 0 \oplus Z, \quad (1)$$

where Z and X are Pauli matrices. M_2 has a zero eigenvalue and is therefore a non-invertible operator whereas M_1 is both Hermitian and unitary with eigenvalues ± 1 (the -1 eigenvalue is doubly degenerate). It is easy to see that M_1 and M_2 anti-commute. Note also that $M_1^2 = 1$ and $M_2^3 = M_2$.

The stabilizers for this code are the vertex operators A_v attached to each vertex v , and plaquette operators B_f attached to each face f , which are defined as follows:



$$A_v = \begin{array}{c} \text{---} M_1 \text{---} \\ | \\ M_1 \text{---} v \text{---} M_1 \\ | \\ M_1 \text{---} \end{array}, \quad B_f = \begin{array}{c} M_2 \\ \bullet \\ \square \\ \bullet \\ M_2 \end{array} \quad (2)$$

Since A_v and B_f either do not overlap or overlap on two edges, they commute as M_1 and M_2 anti-commute. Thus

$$[A_v, A_{v'}] = [B_f, B_{f'}] = [A_v, B_f] = 0. \quad (3)$$

The Hamiltonian is the sum of these mutually commuting stabilizers:

$$H = - \sum_v A_v - \sum_f B_f. \quad (4)$$

The set of operators generated by products of $\{A_v\}$ and $\{B_f\}$ thus form a commutative monoid which we will denote as S . However, this is not the full stabilizer commutative monoid consisting of symmetry operations under which any ground state is left invariant, as will be discussed soon. Restriction of our model to the lower two-dimensional subspace on each edge (on which M_1 acts as X and M_2 acts as Z) gives the \mathbb{Z}_2 -toric code [30].

A. Ground states have topological degeneracy

A ground state of this system will be the simultaneous eigenstate of all A_v and B_f with the highest possible eigenvalues, namely $+1$, so that the energy is minimized. Thus any ground state

can be written in the form:

$$|G\rangle = \mathcal{P}_0 |s\rangle \quad (5)$$

where $|s\rangle$ is a suitable seed state and \mathcal{P}_0 is the product of projectors P_v and P_f , which projects to the +1 eigenstate sector of A_v and B_f , respectively, i.e.

$$P_v = \frac{1}{2}(1 + A_v), \quad P_f = \frac{1}{2}(B_f + B_f^2), \quad \mathcal{P}_0 = \prod_v P_v \prod_f P_f. \quad (6)$$

By construction, \mathcal{P}_0 is the projector to the subspace spanned by *all* groundstates. The degeneracy of the ground states (GSD) can be obtained simply by computing $\text{Tr}(\mathcal{P}_0)$, i.e. the rank of \mathcal{P}_0 . This can be readily done as $\text{Tr}(M_2) = \text{Tr}(M_1 M_2) = \text{Tr}(M_1 M_2^2) = 0$ implies that

$$\begin{aligned} \mathcal{P}_0 = \frac{1}{2^{|v|2|f|}} \prod_f B_f + \frac{1}{2^{|v|2|f|}} \prod_f B_f^2 + \frac{1}{2^{|v|2|f|}} \prod_v A_v \prod_f B_f + \frac{1}{2^{|v|2|f|}} \prod_v A_v \prod_f B_f^2 \\ + \text{traceless terms}, \end{aligned} \quad (7)$$

where $|v|$ and $|f|$ denote the number of vertices and faces on the lattice. Assuming that the lattice is a tessellation of a compact surface, we readily obtain $\prod_v A_v = I$ which further implies that

$$\mathcal{P}_0 = \frac{2}{2^{|v|2|f|}} \prod_f B_f + \frac{2}{2^{|v|2|f|}} \prod_f B_f^2 + \text{traceless terms}. \quad (8)$$

Both the terms $\prod_f B_f$ and $\prod_f B_f^2$ correspond to M_2^2 acting on each edge of the lattice (since $M_2^4 = M_2^2$). Therefore,

$$\mathcal{P}_0 = \frac{4}{2^{|v|2|f|}} \prod_e M_2^2 + \text{traceless terms}. \quad (9)$$

Since $\text{Tr} M_2^2 = 2$, we finally obtain (with $|e|$ denoting the number of edges of the lattice):

$$\text{GSD} = \text{Tr}(\mathcal{P}_0) = \text{Tr} \left(4 \frac{1}{2^{|v|2|f|}} \prod_e M_2^2 \right) = 4 \frac{2^{|e|}}{2^{|v|2|f|}} = 2^{2+|e|-|v|-|f|} = 2^{2-\chi} = 2^{2g}. \quad (10)$$

Above we have used the standard expression for the Euler characteristic of the closed surface $\chi = |v| + |f| - |e|$ in terms of its genus g , namely $\chi = 2 - 2g$. The model has therefore the same GSD as that of the toric code (where a similar but much shorter trace calculation yields the same answer elegantly [49]).

B. Symmetries: stabilizer monoid, annihilator monoid and logical operators

To understand the different types of symmetries of the model, we should look for operators which commute with the Hamiltonian and study their actions on the ground states. The monoid

S generated by $\{A_v\}$ and $\{B_f\}$ forms only a part of the symmetries which leave any ground state invariant. Since, $A_v P_v = P_v$ (as $A_v^2 = 1$) and $B_f P_f = P_f$ (since $B_f^3 = B_f$ and $B_f^4 = B_f^2$) we obtain

$$A_v \mathcal{P}_0 = B_f \mathcal{P}_0 = \mathcal{P}_0 \quad (11)$$

implying that any ground state is invariant under the action of any A_v and any B_f (note that $\mathcal{P}_0 |G\rangle = |G\rangle$ for any ground state $|G\rangle$ as \mathcal{P}_0 by construction is the projector to the subspace spanned by all ground states).

We can readily form the full stabilizer monoid S_M which includes all symmetries that leave any ground state invariant by including more generators which are namely,

- $M_{2,e}^2$ acting on any single edge e of the lattice (note that M_2^2 commutes with M_1 so $M_{2,e}^2$ should commute with the Hamiltonian), and
- loop operators C_{L_c, M_2} denoting M_2 acting on each edge of a contractible loop L_c (note that any such loop operator can overlap with a vertex operator non-trivially on a pair of edges, and will therefore commute with any vertex operator and thus with the Hamiltonian).

It is easy to see that since $M_2^2 = \text{diag}(0, 1, 1)$ and it commutes with the vertex operators, we have $M_{2,e}^2 \mathcal{P}_0 = \mathcal{P}_0$. For any contractible loop L_c , we can multiply all the plaquette operators B_f enclosed by this loop producing C_{L_c, M_2} at the boundary times a product of $M_{2,e}^2$ on all edges enclosed by the loop. Since any B_f and any $M_{2,e}^2$ leaves any ground state invariant, it follows that C_{L_c, M_2} leaves the ground state invariant as well provided that L_c is a contractible loop.

Unlike the case of the toric code, the set of symmetries which leave any ground state invariant is a commutative monoid (S_M), and not an Abelian group. Furthermore, S_M is not generated solely by the local operators, namely $\{A_v\}$ and $\{B_f\}$, as in the toric code, but also by non-local operators, namely $\{C_{L_c, M_2}\}$ of arbitrary sizes. We note that $\{B_f\}$ and $\{C_{L_c, M_2}\}$ are non-invertible since they have zero eigenvalues. However, it is also easy to see that, when restricted to the subspace spanned by the ground states, S_M is actually the same stabilizer group as in the case of the toric code, and is generated by the same elementary vertex and plaquette operators of the latter (composed of X and Z acting on each edge of the vertex or plaquette, respectively). Nevertheless, we will see that the non-invertible elements especially the contractible M_2 loops $\{C_{L_c, M_2}\}$, which are part of the stabilizer monoid, will give rise to striking non-commutative and non-Abelian features in the fusion rules involving fractonic defects.

Logical operators are symmetries which have non-trivial actions on the ground states without annihilating them. These are operators O that commute with all A_v and B_f (and thus with the

Hamiltonian and \mathcal{P}_0), but $OP_0 \neq \mathcal{P}_0$ and $OP_0 \neq 0$. The set of these operators are generated by non-contractible loop operators $C_{L_{nc}}$ denoting the product of M_2 acting on each edge of a non-contractible loop L_{nc} on the lattice, and $C_{\tilde{L}_{nc}}$ denoting the product of M_1 acting on each edge of a non-contractible loop \tilde{L}_{nc} in the dual lattice. The total number of generators are thus $4g$. See Figs. 1 and 2 for an illustration of the logical operators on a torus. These logical operators give a simple recipe for obtaining the 2^{2g} groundstates. Let us choose the seed state $|S\rangle$ to be

$$|S\rangle = \bigotimes_e \prod_e \begin{pmatrix} 0 \\ 1 \\ 0 \end{pmatrix} \quad (12)$$

which is the +1 eigenstate of any $M_{2,e}$ and any B_f . Therefore, one ground state is

$$|G_1\rangle = \mathcal{P}_0 |S\rangle = \prod_v P_v |S\rangle. \quad (13)$$

On the torus ($g = 1$), as for instance, there are two independent non-contractible dual loops, placed on a A cycle and a B cycle, respectively, and therefore two independent $C_{\tilde{L}_{nc}}$, which we denote as \tilde{C}_A and \tilde{C}_B that cannot be transformed to each other via multiplication of (multiple) A_v . (The latter does not affect any groundstate as we have noted already.) Therefore, we get three other ground states which are

$$\begin{aligned} |G_2\rangle &= \prod_v P_v \tilde{C}_A |S\rangle = \tilde{C}_A \mathcal{P}_0 |S\rangle, & |G_3\rangle &= \prod_v P_v \tilde{C}_B |S\rangle = \tilde{C}_B \mathcal{P}_0 |S\rangle, \\ \text{and } |G_4\rangle &= \prod_v P_v \tilde{C}_A \tilde{C}_B |S\rangle = \tilde{C}_A \tilde{C}_B \mathcal{P}_0 |S\rangle. \end{aligned} \quad (14)$$

More generally, we will obtain 2^{2g} groundstates obtained from the 2^{2g} possible products of $2g$ non-contractible dual loop operators (including the identity) acting on the *canonical* groundstate $\mathcal{P}_0 |S\rangle$.⁶ Note that $C_{L_{nc}}$ keeps our chosen seed state invariant and cannot be used to generate any other groundstate. However, with a different choice of seed state we would have needed a different set of $2g$ logical operators for generating all the groundstates.

In fact, when the action of the logical operators is restricted to the subspace spanned by the ground states, they reduce to the logical operators of the toric code; $C_{L_{nc}}$ reduces to the products of Z s acting on each edge of the non-contractible loop L_{nc} while $C_{\tilde{L}_{nc}}$ reduces to the products of X s acting on each edge of the dual non-contractible loop \tilde{L}_{nc} . Therefore, on the subspace generated

⁶ In the general case, we cannot consider a square lattice as it cannot tile a sphere or a compact Riemann surface with genus greater than 1. Our model nevertheless can be defined on an arbitrary tiling of any Riemann surface.

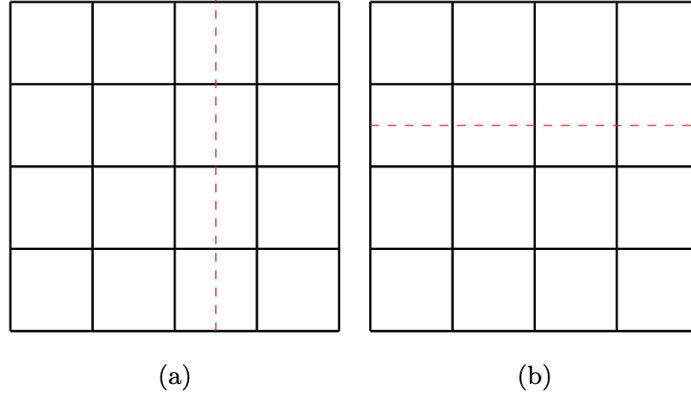


FIG. 1. (a) A non-contractible dual M_1 loop operator along the A cycle of the torus \tilde{C}_A , where we act with M_1 on every edge that is cut by the dotted line. (Note that periodic boundary conditions have been imposed on the square.) (b) A non-contractible dual M_1 loop operator along the B cycle of the torus, \tilde{C}_B .

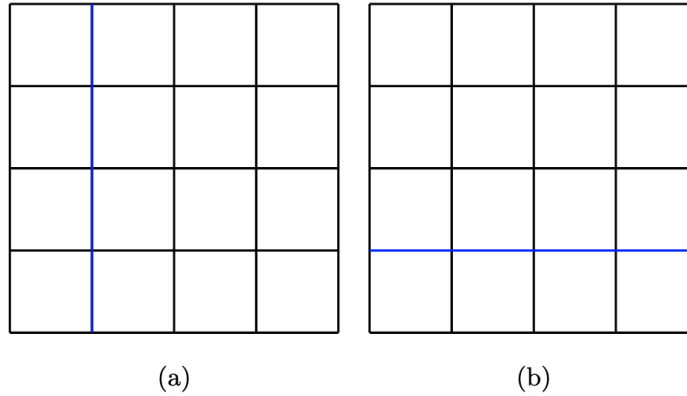


FIG. 2. (a) A non-contractible M_2 loop operator along the A cycle of the torus C_A , where we act with M_1 on every edge that is cut by the dotted line. (Note that periodic boundary conditions have been imposed on the square.) (b) A non-contractible M_2 loop operator along the B cycle of the torus, C_B .

by the ground states, the logical operators can be identified with the normal subgroup formed by the quotient of the full symmetry group by the stabilizer group.

We will see that when restricted to the full sector of states that can decay to a ground state in presence of local perturbations (and composed of mobile electric and magnetic charges), the symmetries, which form the stabilizer monoid and the set of logical operators, act as unitary transformations (representing the action of \mathbb{Z}_2). However, outside of this sector, the stabilizer monoid and the logical operators are not necessarily invertible.

Interestingly, K_e which denotes the action of $K = \text{diag}(1, 0, 0)$ on an edge e annihilates any ground state, and as we will see also the full sector of states that can decay to a ground state in

presence of local perturbations. Since $K M_2 = 0$, it follows that $K_e \mathcal{P}_0 = 0$. K_e is a symmetry as it commutes with both M_1 and M_2 , and thus with the Hamiltonian. One can actually define an annihilator monoid S'_M , which is the set of all symmetries which annihilate any ground state and also the full sector of states that can decay to a ground state in presence of local perturbations. This monoid is generated by $\{K_e\}$, and non-vanishing products of any K_e with any other generator of the symmetries which do not annihilate the ground state. We will show that excited states with fractonic defects can also be eigenstates of K_e with vanishing/non-vanishing eigenvalues depending on the edge e where it is supported.

III. THE EXCITED STATES

A. Deconfined excitations

The deconfined excitations of this model are similar to that of the toric code. Consider a string operator, E_{v_1, v_2} , which denotes the action of M_2 on each edge of a connected path on the lattice starting at the vertex v_1 and ending at the vertex v_2 . See Fig. 3 for an illustration of such a string operator of the smallest length. This string commutes with all vertex operators intersected by this path except A_{v_1} and A_{v_2} . It anti-commutes with both A_{v_1} and A_{v_2} , and therefore

$$E_{v_1, v_2} P_v = \begin{cases} P_v^\perp E_{v_1, v_2}, & \text{if } v = v_1 \text{ or } v = v_2, \\ P_v E_{v_1, v_2}, & \text{otherwise,} \end{cases}$$

where $P_v^\perp = (1/2)(1 - A_v)$ is the projector to the -1 eigensector of A_v . Consequently, for a generic seed state $|s\rangle$,

$$\begin{aligned} |v_1, v_2\rangle &= E_{v_1, v_2} \mathcal{P}_0 |s\rangle = \mathcal{P}_{v_1, v_2} E_{v_1, v_2} |s\rangle, \text{ with} \\ \mathcal{P}_{v_1, v_2} &= P_{v_1}^\perp P_{v_2}^\perp \prod_{v \neq v_1, v_2} P_v \prod_f P_f \end{aligned} \quad (15)$$

It is easy to see that \mathcal{P}_{v_1, v_2} is the projector to the subspace with energy $+4$ above the groundstate in which two vertices, namely v_1 and v_2 are *excited*. $|v_1, v_2\rangle$ is thus an energy eigenstate.

We can excite vertices only in pairs via action of such string operators E_{v_1, v_2} on a ground state (which as discussed before always takes the form $\mathcal{P}_0 |s\rangle$). It can be explicitly checked that the rank of the projector which projects to states with an odd number of excited vertices is zero. As for instance,

$$\text{Tr}(\mathcal{P}_{v_1}) = 0, \text{ where } \mathcal{P}_{v_1} = P_{v_1}^\perp \prod_{v \neq v_1} P_v \prod_f P_f \quad (16)$$

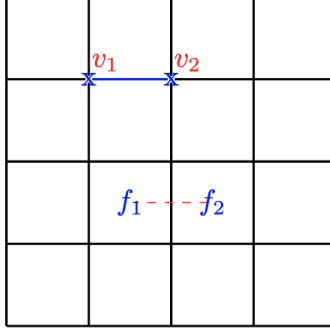


FIG. 3. The smallest M_1 string (dashed red) excites two face operators at the faces $f_{1,2}$. The smallest M_2 string (blue) excites two vertex operators at the vertices $v_{1,2}$.

Furthermore, the energy eigenvalue of $|v_1, v_2\rangle$ does not depend on the length of the string operator E_{v_1, v_2} which creates it by acting on the ground state $\mathcal{P}_0 |s\rangle$. Thus such vertex excitations are deconfined. Following the terminology used in the context of the toric code, we will call these *electric* excitations which always exist in pairs in this sector of purely deconfined excitations.

The other deconfined excitations are created by the dual string operators \tilde{E}_{f_1, f_2} which denotes the action of M_1 on each edge of the real lattice intersected by a connected path in the dual lattice starting at face f_1 and ending at face f_2 . See Fig. 3 for an illustration of such a dual string operator of the smallest length. It is easy to see that it anti-commutes with only two plaquette operators, namely B_{f_1} and B_{f_2} , and commutes with any other plaquette operator. Therefore,

$$\tilde{E}_{f_1, f_2} P_f = \begin{cases} P_f^{\perp, -} \tilde{E}_{f_1, f_2}, & \text{if } f = f_1 \text{ or } f = f_2, \\ P_f \tilde{E}_{f_1, f_2}, & \text{otherwise,} \end{cases}$$

where $P_f^{\perp, -} = (1/2)(-B_f + B_f^2)$ is the projector to the -1 eigensector of B_f . Consequently,

$$\begin{aligned} |f_1, f_2\rangle &= \tilde{E}_{f_1, f_2} \mathcal{P}_0 |s\rangle = \mathcal{P}_{f_1, f_2}^- \tilde{E}_{f_1, f_2} |s\rangle, \text{ with} \\ \mathcal{P}_{f_1, f_2}^- &= \left(\prod_v P_v \right) P_{f_1}^{\perp, -} P_{f_2}^{\perp, -} \prod_{f \neq f_1, f_2} P_f \end{aligned} \quad (17)$$

We note that \mathcal{P}_{f_1, f_2}^- is a projector to the energy eigensector with energy $+4$ above the groundstate in which only the two faces, namely f_1 and f_2 are excited. $|f_1, f_2\rangle$ is thus an energy eigenstate.

We can create such excited states with pairs of faces excited by the action of dual string operators on a ground state. Following the toric code terminology, these are the deconfined *magnetic* excitations whose energy is independent of the length of the dual string creating them. The identities

$$E_{v_1, v_2} E_{v_2, v_3} = E_{v_1, v_3}, \quad \tilde{E}_{f_1, f_2} \tilde{E}_{f_2, f_3} = \tilde{E}_{f_1, f_3} \quad (18)$$

are obvious. Furthermore, consider any pair of strings E_{v_1, v_2} or a pair of dual strings \tilde{E}_{f_1, f_2} with the same endpoints and such that the (dual) strings in the pair are homological to each other. Their combined action is a contractible loop or dual loop which is part of the symmetry monoid S_M that leaves any ground state invariant. Together these imply that we can move one or both of the endpoints of a string or a dual string operator via actions of operators of finite length and without any extra energy cost (meaning that by action of other (dual) string operators one can translate the end points of any (dual) string without creating more excitations). Thus the deconfined electric and magnetic excitations are mobile.

The whole sector of deconfined excitations (just like the ground states as mentioned before) is annihilated by the action of K_e involving the action of the the matrix $K = \text{diag}(1, 0, 0)$ acting on any edge e of the lattice, since only the subspace spanned by $(0, 1, 0)$ and $(0, 0, 1)$ on each edge (the toric code subspace) appear in such states. The dynamics in this sector mimics the toric code exactly. For the same reasons, all elements of the stabilizer monoid and the logical operators act as unitary transformations representing the action of \mathbb{Z}_2 on this sector of states.

B. Fractonic excitations: Confined immovable defects and their internal states

This model admits another class of excitations that are immobile (fractonic) and confined. Note that for the deconfined excitations, the excited plaquettes have -1 eigenvalues for the respective face operators B_f . Here we will study the excitations in which the vertices are not excited (i.e. all A_v have $+1$ eigenvalues) but in which some of the face operators B_f have zero eigenvalues (zero fluxes), and show that such excitations are fractonic and confined.

The projector to the zero eigenvalue sector of B_f is $P_f^{\perp, 0} = (1 - B_f^2)$. Let us consider the following projector $\mathcal{P}_{f_1, f_2, \dots, f_n}^d$ to the energy eigenstate sector in which n faces f_1, f_2, \dots, f_n are excited to zero eigenvalues:

$$\mathcal{P}_{f_1, f_2, \dots, f_n}^d = \left(\prod_v P_v \right) P_{f_1}^{\perp, 0} P_{f_2}^{\perp, 0} \dots P_{f_n}^{\perp, 0} \prod_{f \neq f_1, f_2, \dots, f_n} P_f. \quad (19)$$

As illustrated in Appendix A, $\text{Tr}(\mathcal{P}_{f_1, f_2, \dots, f_n}^d) = 0$ if any of the faces f_i with zero flux does not share an edge with another face f_j with zero flux ($i, j = 1, \dots, n$ and $i \neq j$). Thus any isolated zero flux face excitation cannot exist. The trace (and thus the rank of the projector) is non-vanishing otherwise implying existence of eigenstates with energy $+n$ above the ground state. See Fig. 4 for an illustration. Which operator creates such excitations? Let us consider the simplest excitation of this type in which two adjacent faces f_1 and f_2 have zero fluxes (see Fig. 4 (a)). The rank of

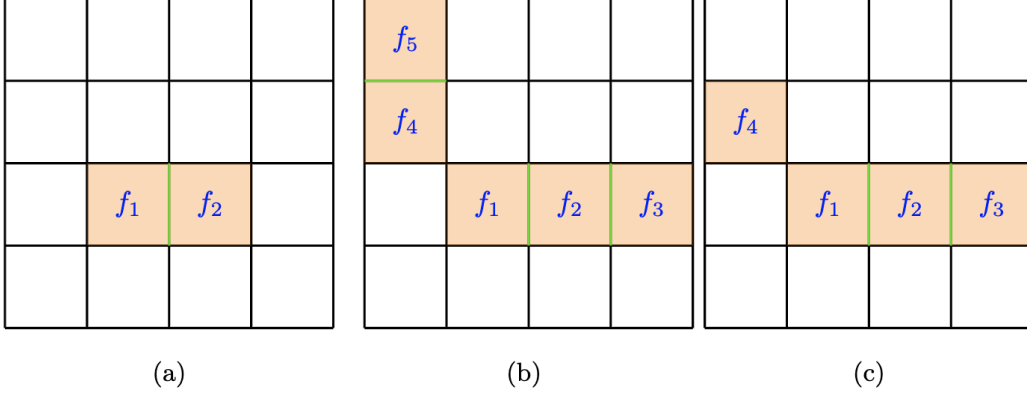


FIG. 4. (a) Simplest allowed configuration. Green edge indicates the action of M_3 . (b) Example of an allowed configuration where all excited faces share an edge with at least one other excited face. (c) Example of a disallowed configuration where f_4 is excited but is not connected with any other face excitations.

the projector to this energy eigenstate sector is 2^{2g} (see Appendix A). Therefore, it is natural to postulate that these energy eigenstates can be created by an operator M_3 supported on the edge e' shared by f_1 and f_2 acting on any of the 2^{2g} groundstates.

To construct M_3 explicitly, it is convenient to consider the seed state $|S\rangle$ defined in Eq. (12) which is a +1 eigenstate of all B_f . Demanding that M_3 commutes with M_1 and that it rotates the +1 eigenstate of M_2 to the 0 eigenstate of M_2 , we obtain

$$M_3 = \begin{pmatrix} 0 & 1 & -1 \\ 0 & 0 & 0 \\ 0 & 0 & 0 \end{pmatrix} \quad (20)$$

Note M_3 endowed with the properties that we have demanded is not unique, however we will discuss the rationale for the above choice in the following section. For the present purposes, any other choice of M_3 would also work. Let us denote the operator M_3 supported on an edge e' as $M_{3,e'}$. It follows that with $|S\rangle$ given by Eq. (12), we obtain

$$\begin{aligned} |E\rangle &= M_{3,e'} \mathcal{P}_0 |S\rangle = M_{3,e'} \prod_v P_v \left(\bigotimes_e \prod_e \begin{pmatrix} 0 \\ 1 \\ 0 \end{pmatrix}_e \right) = \prod_v P_v M_{3,e'} \left(\bigotimes_e \prod_e \begin{pmatrix} 0 \\ 1 \\ 0 \end{pmatrix}_e \right), \\ &= \prod_v P_v |S'\rangle, \text{ with } |S'\rangle = \left(\begin{pmatrix} 1 \\ 0 \\ 0 \end{pmatrix}_{e'} \bigotimes_{e \neq e'} \prod_e \begin{pmatrix} 0 \\ 1 \\ 0 \end{pmatrix}_e \right). \end{aligned} \quad (21)$$

The second equality above follows from the fact that $|S\rangle$ is left invariant by any P_f . The third and

fourth equalities follow from the defining properties of M_3 that it commutes with M_1 , and it takes the $+1$ eigenstate of M_2 to the 0 eigenstate of M_2 , respectively (thus any such M_3 which can be different from the choice in Eq. 20 will also work). We can show that $|E\rangle$ is an eigenstate of the Hamiltonian. The final form of $|E\rangle$ implies that it is a $+1$ eigenstate of all A_v since the product of all P_v acts on the extreme left. Furthermore, as B_f commutes with all A_v , we obtain

$$B_f |E\rangle \begin{cases} = |E\rangle & \text{if the face } f \text{ does not have the edge } e', \\ = 0, & \text{otherwise} \end{cases} . \quad (22)$$

Thus $|E\rangle$ is an energy eigenstate in which all A_v have $+1$ eigenvalues, and all faces B_f have $+1$ eigenvalues except for the two faces f_1 and f_2 shared by the edge e' (on which the action of M_3 has been supported). The other independent states in the image of \mathcal{P}_{f_1, f_2}^d can be created by the action of $M_{3, e'} O$ (or $O M_{3, e'}$) acting on $\mathcal{P}_0 |S\rangle$ where O is a logical operator which is made out of products of M_1 acting on each edge of a non-contractible loop on the dual lattice, or a product of such logical operators. We can thus account for the 2^{2g} degeneracy of the smallest element of the sector with two adjacent zero flux faces.

As evident from the result of the explicit computation of the rank of the projector $\mathcal{P}_{f_1, \dots, f_n}^d$, the excitation pair created via the action of M_3 on a single edge is confined. As for instance, consider the pair of adjacent zero flux faces f_4 and f_5 in Fig. 4(b). This pair cannot be separated without creating additional zero flux excitations since two separated face excitations with zero fluxes are disallowed. The separation of a pair of adjacent zero flux excitations can be achieved only by a creation of a string of zero flux excitations between them costing energy proportional to the length of the string. This is the hallmark of confinement.⁷

Furthermore, these zero flux excitations are fractonic. A pair of deconfined electric and magnetic charges are mobile since both endpoints of the string can be moved without any energy cost by action of operators with finite support as noted before. However, a pair of adjacent zero flux faces f_1 and f_2 cannot be moved to another pair of adjacent faces f_3 and f_4 via the action of any local operator since M_3 is non-invertible (it is easy to check that any choice of M_3 satisfying the defining properties is non-invertible). The fractonic nature of such zero flux excitations is thus more extreme than those of other stabilizer code models like the X-cube model introduced in [33]. In the latter case, translation of a fractonic excitation can be implemented by actions of local

⁷ Recently, it has been pointed out that an Hamiltonian with fractonic excitations can be obtained by integrating out a confining gauge field [50]. A similar phenomena also occurs for the fluxes in a \mathbb{Z}_2 -toric code with matter fields on the vertices as discussed in [51].

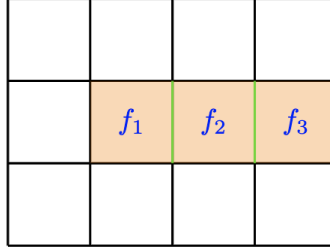


FIG. 5. Three faces $f_{1,2,3}$ are excited to the zero eigenstate.

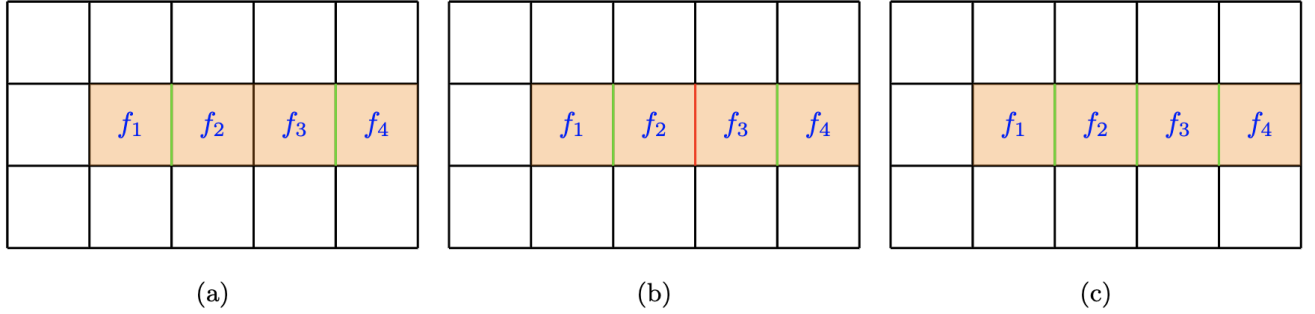


FIG. 6. Three states with the faces $f_{1,2,3,4}$ excited to the zero eigenvector. Green lines indicate the action of M_3 on the edge and red lines denote the action of M_1 .

operators (supported within a subregion of the lattice) although with energy costs, but in our case such translations are simply impossible.

Another remarkable property of these fractonic confined excitations is that these have internal degrees of freedom when there are sufficient number of zero flux faces forming clusters with specific geometric shapes.

Consider three zero flux excitations f_1 , f_2 and f_3 forming a linear chain as shown in Fig. 5. The trace of the corresponding projector $\mathcal{P}_{f_1, f_2, f_3}^d$ is 2^{2g} (see Appendix A) implying that there is no internal degree of freedom for this zero flux cluster. These states are created via the product of M_3 supported on the two internal edges (i.e. that shared between f_1 and f_2 and that shared between f_2 and f_3 , respectively) acting on one of the 2^{2g} groundstates. The conclusion is the same if these three adjacent zero flux states is L-shaped instead of being a linear chain. However, the case with four zero flux face excitations is more non-trivial. Consider four face excitations f_1 , f_2 , f_3 and f_4 forming a linear chain as shown in Fig. 6. The rank of the corresponding projector $\mathcal{P}_{f_1, f_2, f_3, f_4}^d$ is 3×2^{2g} . The factor of 3 can be accounted for by 3 distinct operators as shown in Fig. 6. Firstly, after the action of M_1 on an edge shared by two zero flux faces, the latter remain zero flux faces. Since $M_3 M_1 = -M_3 = M_3 M_1$, therefore M_1 acting on an edge where the action of M_3 is supported

cannot create a new state. Furthermore, acting with M_1 on any other internal edge of a zero flux face cannot change the eigenvalue (equal to zero) of the corresponding B_f operator since one edge of the face, where M_3 acts, is already in the zero eigenstate of M_2 . However, a new internal state of the defect may be generated by such an action.⁸ The factor of 3 in the degeneracy arises from the 3 possible actions of M_3 and M_1 as shown in Fig. 6. (The central internal edge can have identity, M_1 or M_3 acting on it while both the other two internal edges must support the action of M_3 so that four zero flux face excitations are created as shown in the figure.) Remarkably, a linear chain of four zero flux face excitations (with no vertex excitations) thus effectively acquires a spin 1 internal degree of freedom.

We can also construct a configuration of four zero flux faces forming a square as shown in Fig. 7. As shown in Appendix A, the rank of the corresponding projector $\mathcal{P}_{f_1, f_2, f_3, f_4}^d$ is 9×2^{2g} implying that this zero flux configuration has 9 internal states (and thus effectively a spin 4 internal degree of freedom).

The 9 operators which can act on one of the 2^{2g} groundstates to create these linearly independent 9×2^{2g} excited states involving inequivalent combinations of M_3 and M_1 are shown in Fig. 7. Since A_v leaves any ground state invariant, if two operators O and O' are related by $O = O'A_v$, then they will create the same state acting on any groundstate and will be equivalent (for a precise definition of equivalence see the following section). Using $M_1^2 = 1$ and $M_1M_3 = -M_3 = M_3M_1$, we thus obtain only two inequivalent operators involving a product of the action of M_3 on two internal edges and that of M_1 on another internal edge. Similarly, the action of M_1 on an internal edge does not produce any new state if M_3 acts on the remaining three internal edges. We thus explicitly obtain the 9 operators which together with the logical operators generate all the excited states in which four zero flux face excitations form a square and in which no vertex is excited.

Unlike other stabilizer code models, fractonic zero flux face configurations (defects) do not acquire partial or complete mobility when they combine to form bigger clusters. This implies that our fractonic model is not of type I. However, as demonstrated above, fractonic defects acquire internal degrees of freedom where the number of internal states depends on the geometry and size of the configuration. These internal states are generated by the different combinations of M_3 and M_1 that can be supported on the internal edges (always accompanied by with sufficient number of M_3 supported on appropriate internal edges creating the zero flux configuration) acting on any vacuum state.

⁸ Note that M_1 cannot act on any of the boundary edges of the orange defect region since that will excite the adjoining face outside the region to the -1 eigenvalue. This actually creates magnetic monopoles as discussed in detail in the following subsection.

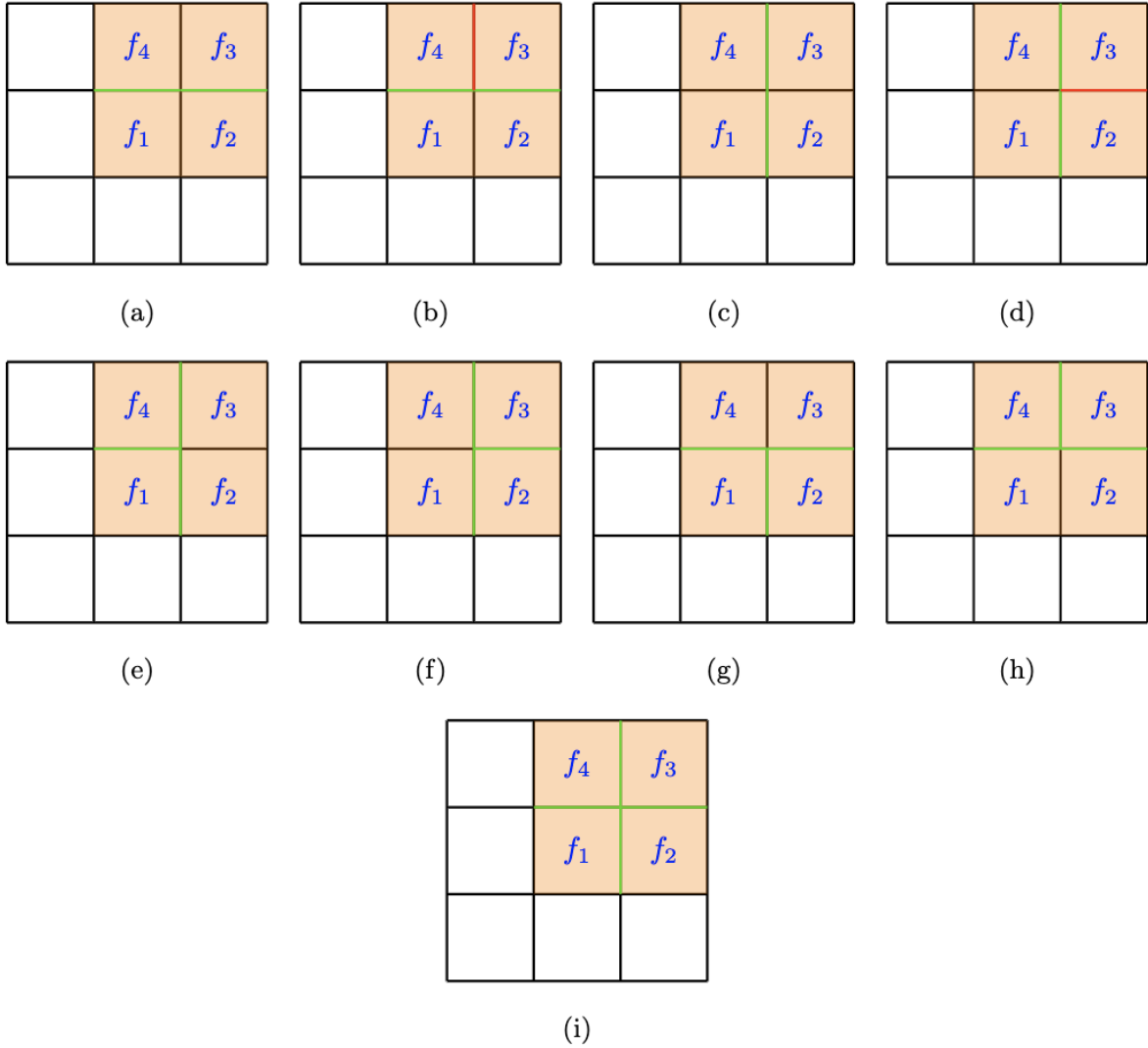


FIG. 7. Nine distinct configurations with four face excitations arranged in a square. Solid green lines indicate the action of M_3 and red lines indicate the action of M_1 .

K_e involving the action of the the matrix $K = \text{diag}(1, 0, 0)$ supported on any edge e of the lattice are symmetries that have interesting actions on the states featuring fractonic defects. If it acts on any edge except for the edges supporting the action of M_3 needed to create the fractonic defect configuration, the state is annihilated. Otherwise the state is an eigenstate of this symmetry. Therefore, the action of K_e can detect not only the location of the fractonic defects, but also partial information of how it is created via the action of M_3 supported on the internal edges of the configuration. Similarly, M_2^2 acting on a single edge will annihilate any defect configuration if it overlaps with any edge where M_3 needs to act to create the defect configuration from a ground state.

The case of a contractible M_2 loop which is part of the stabilizer monoid is the most interesting. Consider a big M_2 contractible loop which encircles the defect region with a linear arrangement of four zero flux faces as in Fig. 6 such that it intersects the defect region only on the middle internal edge. Depending on whether 1 or M_1 or M_3 acts on this edge to create the internal state of the defect, the eigenvalue of the M_2 loop would be 1, -1 or 0. Therefore, the measurement of this M_2 loop together with other such contractible M_2 loops can reveal the internal state of the defect along with its location.

C. Deconfined stuff and fractons: Magnetic monopoles and restricted electric charges

Here we analyze the general case where we can have vertex excitations, i.e. vertices v with A_v eigenvalues -1 together with face excitations of both types, i.e. faces with B_f eigenvalues which can be either -1 or 0. Such excited states involve both electric and magnetic charge excitations and zero flux configurations (defects). Since we have already studied which operators can create such excitations by acting on a vacuum state, we can readily deduce how such general excitations can be created. Remarkably, we find that the mobile excitations, i.e. the electric and magnetic charges change their nature in the presence of the fractonic defect configurations.

Firstly, a fractonic defect configuration can absorb any of the magnetic charges of a pair (created by a dual string) and thus create magnetic monopoles. Consider the configuration shown in Fig. 8. Here M_1 acts on the outer edge of a fractonic defect configuration. This is the shortest dual string connecting two adjacent faces, but with one of the faces in the defect region. Here the action of M_1 excites only the face exterior to the defect region to -1 eigenvalue of B_f . As discussed before, the B_f eigenvalue of the other face within the defect region remains zero. This implies that we have created a magnetic monopole attached to the defect region.

More generally, we can consider any dual string \tilde{E}_{f_1, f_2} with one of the terminal faces, as for instance f_2 , coinciding with a face at the border of a defect region with zero flux. It is easy to see that in such a case only the face f_1 will be excited to -1 eigenvalue of B_f , whereas the face f_2 will still have zero flux. In the presence of a zero flux defect configuration, we can thus create a magnetic monopole (where a single face is excited to -1 eigenvalue) anywhere outside the defect configuration.

Furthermore, if the dual string \tilde{E}_{f_1, f_2} has one of the terminal faces, as for instance f_2 , not at the border but within a defect region with zero flux, then via the action of M_1 on an internal edge, it may modify the internal state of the defect while creating a magnetic monopole (at the face

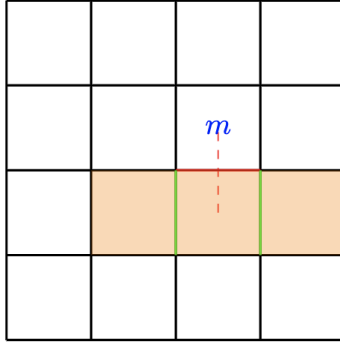


FIG. 8. The defect region (orange) absorbs one magnetic charge creating an isolated magnetic charge m . Note that the other face connected to the edge with the red M_1 operator is not excited to the -1 eigenvector since that face is already in the defect region and excited to the 0 eigenvalue.

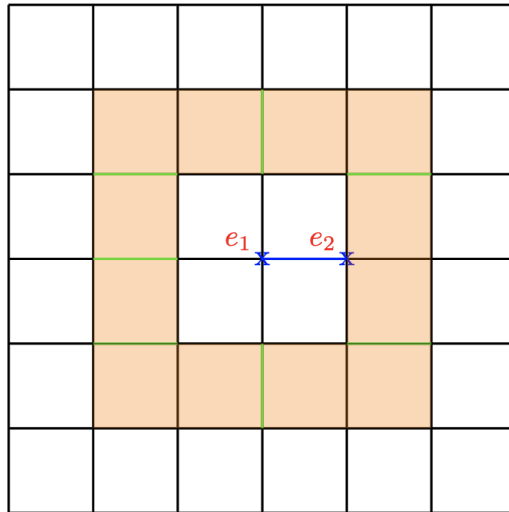


FIG. 9. The defect region (orange) contains a pair of electric charges $e_{1,2}$ created by the action of M_2 (blue) on an edge. These charges have restricted mobility and can only be moved along paths that don't include the green edges with the action of M_3 .

f_1) outside the defect configuration. Therefore, dual string operators \tilde{E}_{f_1, f_2} (magnetic charges) interact non-trivially with zero flux defect configurations since one of the endpoints of a dual string can be absorbed by the defect configuration with or without altering the internal state of the latter.

To analyze the nature of electric charge excitations in presence of zero flux defect configurations, we need to be aware that M_2 and M_3 do not commute, and that $(M_2 M_3)_e |G\rangle = M_{2,e} |E\rangle = 0$ since the action of M_3 supported on an edge e on any ground state brings the state of the edge to the 0 eigenstate of M_2 (see Eq. 20). Let us consider operators creating energy eigenstates by acting on the ground state such that those creating zero flux configurations (the actions of M_3 and M_1 on

various edges) are to the right of the string operators E_{v_1, v_2} which create pairs of electric charge excitations. In this context, the zero flux configurations act as perfect repellers of electric charges. Consider the configuration shown in Fig. 9. The charges, e_1 and e_2 at the ends of the string can only move along a path on the lattice which does not intersect on any edge where M_3 acts (as otherwise the state is annihilated). Thus electric charges acquire restricted mobility in presence of the zero flux configurations if they are created after the creation of the defect configuration (and the full operator creating the entire configuration is ordered in the way mentioned). *Unlike the magnetic monopole, the electric charge cannot be passed through a defect region along an arbitrary path.* On the other hand, if we allow other operator orderings, then we create hybrid configurations in which vertices within defect configurations can be excited.

We note that such configurations of magnetic monopoles and electric charges external to fractonic defects can retain mobility in their local neighborhoods but full configurations of such types cannot be brought back to the ground state via local operations exactly for the same reasons which apply for the fractonic defects as discussed before. Since, not all (partially) mobile excitations can decay to the ground state in the presence of local perturbations, our model is not of type II. Earlier we have argued that our model is not of type I either.

The most elegant way to capture the full set of excitations is via construction of appropriate superselection sectors and their fusion rules as in the following section. We will find that the model requires the construction of a novel fusion category which is both non-commutative and non-Abelian, and requires including the zero operator for closure.

IV. A NOVEL FUSION CATEGORY: NON-COMMUTATIVE AND NON-ABELIAN

A. An intuitive discussion

Superselection sectors and their products given by the fusion rules are important tools for classifying quantum phases of matter in terms of their fundamental excitations. We will briefly review first how this works for the toric code in an intuitive way and then we will proceed to give formal definitions which generalize the standard constructions in a way that can include non-invertible operators. For this entire section, we will consider a square lattice with a boundary and our statements should be understood in the limiting situation where the lattice is infinite (has infinitely many edges). Our discussion in this subsection will be similar to that in [52] (see also [53, 54]).

Consider a bounded region R in the lattice. Any string operator E_{v_1, v_2} or dual string operator \tilde{E}_{f_1, f_2} will create a pair of magnetic and a pair of electric charge excitations, respectively, acting on the ground state. If $v_1, v_2 \in R$ and $f_1, f_2 \in R$, then the reduced density matrix of these excited states obtained by tracing out the edges in R , will be the same as that of the vacuum (as evident from the explicit expressions (15) and (17)). Such excitations are thus localized in R . Furthermore, these states can be brought back to the ground states by the application of another E_{v_1, v_2} or another \tilde{E}_{f_1, f_2} both of which are entirely supported within R and are homologous to the original string or dual string operators that created these excited states, respectively (although the latter need not be supported entirely within R). Therefore, all such pairs of electric and magnetic charge excitations with the excited faces and vertices, respectively, localized in R , are in the ground state super-selection sector because,

- these excitations can be brought back to a ground state by the action of operators supported within R , and
- the reduced density matrix in the complement of R is the same as that of a ground state.

We emphasize that the above does not imply that these states themselves are created necessarily by operators that are supported within R by their action on ground states. This superselection sector can be referred to be that of 1, the identity operator, which leaves the ground states invariant (we will give a precise definition of equivalence below).

The toric code however is a topological phase where non-local operators of arbitrary length play a fundamental role. Therefore, we expect that other superselection sectors exist and this is indeed the case. Consider a long string or a long dual string with one endpoint at infinity and another in R . This will create a single electric or magnetic charge excitation within R and another electric or magnetic charge excitation which is infinitely far away. It is easy to see that

- for such excited states the reduced density matrix over any region R' , which does not overlap with R , is at finite distance from R and has finitely many edges, is the same as that for a ground state (as evident from (15) and (17)) implying that the excitations are effectively localized in R although the operator creating this excitation is not localized in R , but
- such excited states cannot be brought back to any ground state by the action of any operator which is supported within R .

Such considerations lead us to four superselection sectors which are as follows

- the superselection sector 1 as defined above,
- the superselection sector of e consisting of odd number of non-overlapping long string operators with one of their endpoints in R (and their other endpoints at infinity),
- the superselection sector of m consisting of odd number of non-overlapping long dual string operators with one of their endpoints in R (and their other endpoints at infinity), and
- the superselection sector of d consisting of odd number of long string operators and odd number of long dual string operators with one of their endpoints in R (and their other endpoints at infinity), and non-overlapping with each other.

We note the following:

- Any state can be transformed to any other state within the same superselection sector by the action of an operator localized in R , e.g. the state created by the action of any odd number of long string operators ending at R is equivalent to the state created by the action of a single long string operator ending at R as each can be transformed to the other via the action of string operators localized within R (the reduced density matrices of these two states on any finite bounded region of the lattice are identical).
- Two states belonging to two different superselection sectors cannot be transformed to each other via the action of any operator localized within R .
- All superselection sectors describe excitations effectively localized within R because the reduced density matrix over any finite region R' , which does not overlap with R and is at finite distance from R is the same as that for a ground state although the operators creating the excitations are not necessarily localized in R .

Furthermore, we note that any state in the superselection sector d is the product of an operator which creates a state in superselection sector e with an operator which creates a state in superselection sector m . Here, the product commutes (although the operators themselves may not) since states are defined up to multiplication by phases. Given that the toric code has only four superselection sectors for any bounded region R , it is obvious that we can formalize a multiplication rule, a.k.a. fusion rule, defining operator equivalence classes and a fusion product under which the finite set of equivalence classes is closed.

In what follows, we will give a formal definition of the operator equivalence classes and the fusion rules under which the set of equivalence classes is closed. Our definitions will reproduce

the fusion rules of the toric code but the fusion product in the model of interest in this paper will be non-commutative and we will also need to include the equivalence class of the zero operator to achieve closure. Both of the latter features are novel and are necessitated by the presence of non-invertible operators.

B. Generalization of the fusion category

In order to have a consistent definition of operator equivalence classes that correspond to superselection sectors, we need to first restrict ourselves to the set of operators which generate (excited) eigenstates of the Hamiltonian when they act on ground states, and which are closed under multiplication. Such a set of operators which generate excitations in a finite region R , forms a monoid, which we call the spectral monoid of R , and denote as \mathcal{A}_R . We define it more precisely as below.

Consider a set of operators \mathcal{A}_R corresponding to a bounded sub-region R of the lattice with the following properties:

- **Spectrum generation:** For any $A \in \mathcal{A}_R$, $|A\rangle = A\mathcal{P}_0|S\rangle$ is an energy eigenstate or vanishes for a standard state $|S\rangle$ where \mathcal{P}_0 is the projector to the ground state manifold.
- **Localization of excitations in R :** For any finite subregion R' which has no overlap with R and is at finite distance from R , the reduced density matrix of any non-vanishing state $\text{Tr}_{\overline{R'}}(|A\rangle\langle A|)$ corresponding to an $A \in \mathcal{A}_R$ as mentioned above, should coincide with that of a canonical ground state.⁹($\overline{R'}$ denotes the complement of R' .)
- **Closure:** For any $A, B \in \mathcal{A}_R$, $|AB\rangle = AB\mathcal{P}_0|S\rangle$ is also an energy eigenstate or vanishes.
- **Completeness:** All energy eigenstates localized in R can be generated by a suitable $A \in \mathcal{A}_R$ acting on a ground state.
- **Minimality:** The set \mathcal{A}_R is minimal in the sense that removal of any element from \mathcal{A}_R would lead to a violation of one of the above properties.

\mathcal{A}_R is a monoid since it includes the identity operator, and satisfies closure and associativity under matrix multiplication. We call the set \mathcal{A}_R the spectral monoid of R . Following the discussion in the previous subsection, we note that although the excitations generated by operators in \mathcal{A}_R are localized in R , the operators $A \in \mathcal{A}_R$ are not necessarily supported entirely within R . We also note

⁹ The choice of a specific ground state removes the logical operators from our discussion.

that in a standard QFT with a unique ground state, such operators are the just the set of particle creation and annihilation operators when we consider the whole of space instead of a bounded and finite region R , with \mathcal{P}_0 essentially being the evolution in infinite Euclidean time so that it projects a generic state to the ground state.

We define an equivalence class of operators composing the spectral monoid \mathcal{A}_R as follows. We say that $A \in \mathcal{A}_R$ and $B \in \mathcal{A}_R$ are equivalent, i.e. $A \equiv B$ if and only if there exists operators $C \in \mathcal{A}_R$ and $D \in \mathcal{A}_R$ both of which are entirely supported in R and realize the following conditions

$$AP_0 = CBP_0, \quad \text{and} \quad BP_0 = DAP_0. \quad (23)$$

We also identify the excitations $|A\rangle$ and $|B\rangle$ created by these operators to be in the same superselection sector. It is easy to verify that the above indeed establishes an equivalence relation. We note that C and D are not necessarily inverses of each other, and in fact they can be non-invertible.

The above definition of equivalence class takes into account that there can exist energy eigenstates $|A\rangle$ and $|B\rangle$ with the excited vertices/faces in R such that $|B\rangle$ can be obtained from $|A\rangle$ via the action of an operator supported in R and acting on $|A\rangle$, but *not* vice versa. In this case, $|A\rangle$ and $|B\rangle$ will not belong to the same superselection sector. One simple example of such a situation is an elementary pair of adjacent zero flux states in our model, which can be created by the action of M_3 supported on the shared edge acting on the ground state. This state cannot be brought back to the ground state via the action of any local operator. Therefore, this eigenstate is not in the same superselection sector as the ground state although it can be created by the action of a local operator on the latter.

It is also important to note that unlike in usual models the zero operator (0) needs to be included for closure, since products of operators in \mathcal{A}_R can vanish. In fact, one can readily check from Eq. 20 that $M_3^2 = 0$ (we will discuss soon why the choice of M_3 as given by Eq. 20 follows from the requirement that it is an element of \mathcal{A}_R).

The fusion rules are defined as follows. Let $\mathcal{A}_R^{(i)}$ denote equivalence classes with i ranging from 1 to n . With the symbols \otimes and \oplus , we can write

$$\mathcal{A}_R^{(i)} \otimes \mathcal{A}_R^{(j)} = f_{ij1}\mathcal{A}_R^{(1)} \oplus f_{ij2}\mathcal{A}_R^{(2)} \oplus \cdots \oplus f_{ijn}\mathcal{A}_R^{(n)}, \quad \text{for } k = 1, 2, \dots, n \quad (24)$$

The symbol \otimes on the left hand side implies we are considering arbitrary elements from both $\mathcal{A}_R^{(i)}$ and $\mathcal{A}_R^{(j)}$ and multiplying them, whereas \oplus on the right hand side is an “or” symbol implying that the result of the multiplication is in one of the equivalence classes in \mathcal{A}_R . The fusion rules are specified by f_{ijk} , a.k.a. fusion coefficients, which are either 0 or 1 and denote the absence or

presence of the various classes. Note that f_{ijk} and f_{jik} need not be equal, so the fusion product \otimes could be non-commutative (we will explicitly see this in the context of our model in the following subsection).

Note also that the fusion rules are typically associative, so we expect

$$\sum_m f_{ijm} f_{mkl} = \sum_m f_{iml} f_{jkm}. \quad (25)$$

Although matrix multiplication is associative and \mathcal{A}_R is closed under matrix multiplication by construction, one can readily see that the associativity can fail if one does not generate sufficiently enough number of elements in the equivalence class corresponding to a non-vanishing fusion coefficient of any fusion product. Therefore, the above relation needs to be checked explicitly. We have explicitly checked that associativity holds in our model.

A fusion rule is called non-Abelian if more than one fusion coefficients generated by a fusion product is non-zero. This terminology is derived from the fusion rules of non-Abelian anyons [42, 55].

Another way to define fusion rules is by counting multiplicity, namely allowing each fusion coefficient to be a non-negative integer that counts how many times the corresponding equivalence class appears on the right hand side of the fusion product [42, 43, 55]. However, this involves cumbersome combinatorics with the result depending on the size and geometry on R rather than the microscopic nature of the model itself. Therefore, we refrain from such a computation.

C. Fusion rules of the model

We need to first show that we can define the spectral monoid \mathcal{A}_R for any subregion R on the lattice in our model, and then identify the equivalence classes (superselection sectors) and compute the fusion coefficients.

To define a spectral monoid \mathcal{A}_R , we need to choose M_3 appropriately. The defining properties of M_3 used earlier implied $M_3 M_1 = -M_3 = M_1 M_3$ and that M_3 takes eigenvectors of M_2 with ± 1 eigenvalue to the eigenvector of M_2 with 0 eigenvalue. Such an M_3 can also be of the form

$$M_3 = \begin{pmatrix} 0 & 1 & -1 \\ 1 & 0 & 0 \\ -1 & 0 & 0 \end{pmatrix} \quad (26)$$

instead of that given by Eq. (20). However, for the above choice $M_3^2 = I - M_1$, and therefore M_3^2 supported on a single edge does not produce an energy eigenstate when it acts on any ground

state. This violates the closure property required of \mathcal{A}_R . With M_3 chosen as given by Eq. (20) we are able to obtain a spectral monoid \mathcal{A}_R . To see this let us define M_4 as below

$$M_4 = M_3 \cdot M_2 = \begin{pmatrix} 0 & 1 & 1 \\ 0 & 0 & 0 \\ 0 & 0 & 0 \end{pmatrix} \quad (27)$$

We find that

$$\begin{aligned} M_3 \cdot M_3 &= M_3 \cdot M_4 = M_4 \cdot M_3 = M_4 \cdot M_4 = 0, \\ M_3 \cdot M_1 &= M_1 \cdot M_3 = -M_3, \\ M_4 \cdot M_1 &= -M_1 \cdot M_4 = M_4, \\ M_3 \cdot M_2 &= M_4, \\ M_4 \cdot M_2 &= M_3, \\ M_2 \cdot M_3 &= M_2 \cdot M_4 = 0, \end{aligned} \quad (28)$$

Note that M_4 anti-commutes with M_1 (while we recall that M_3 commutes with M_1). We can readily see that M_4 supported on a single edge will create zero flux face excitations on the two overlapping faces and also excite the two overlapping vertices to -1 eigenvalues of A_v . It is thus a hybrid excitation. Furthermore we recall that any ground state is invariant under the action of M_2^2 supported on a single edge, while $M_1^2 = I$. The product of M_1 and M_2 acting on a single edge creates a hybrid dyonic excitation d in which the two adjacent faces have -1 eigenvalues of B_f and the two adjacent vertices have -1 eigenvalues of A_v . The remaining products are readily deduced. We conclude that the set of operators generated by the action of M_1 , M_2 and M_3 on a single edge indeed forms a monoid each element of which generates an energy eigenstate when it acts on a ground state. It is a complete set as we generate all possible combinations of the eigenvalues of A_v for the two overlapping vertices and eigenvalues of B_f for the two overlapping faces that are different from 1, and it is also a minimal set as M_1 , M_2 and M_3 form a minimal set of generators for the set of operators which can produce all such excitations by acting on a ground state. Finally, this set satisfies closure in the sense mentioned above.

Since the Hilbert space is a tensor product of those of the edges of the lattice, we can finally conclude that *the spectral monoid \mathcal{A}_R is generated by the action of M_1 , M_2 and M_3 on the edges within R , and that of any long string and any long dual string each with one end point within R and another end point at infinity.* The inclusion of the long string and the long dual string into the set of generators is necessary for exactly the same reasons discussed previously in the context of the

toric code (they produce a single electric/magnetic charge excitation entangled with the another electric/magnetic at infinity and this does not violate the requirement of effective localization of the excitation within R as discussed before).

If there are no zero flux face excitations in the region R , then the fusion rules are exactly that of the toric code. There are only three equivalence classes e (electric charge), m (magnetic charge) and d (the dyon) discussed before which have the fusion rules,

$$\begin{aligned}
e \otimes e &= m \otimes m = d \otimes d = 1, \\
e \otimes m &= d = m \otimes e, \\
m \otimes d &= e = d \otimes m, \\
d \otimes e &= m = e \otimes d.
\end{aligned} \tag{29}$$

The representative operators of e and m are a single long string (or an odd number of them) and a single long dual string (or an odd number of them), respectively, each with one endpoint in R and another endpoint at infinity. Note that any even number of e, m in R is equivalent to the identity operator since such excited states can be created and transformed to the vacuum by acting appropriate $M_{1,2}$ strings, and this is captured by the fusion rules $e \otimes e = m \otimes m = 1$. The representative operator in d is a product of one (or odd number of) long string(s) and one (or odd number of) long dual string(s) each with one endpoint in R and another at infinity.

When there are only two adjacent zero flux defect faces in R , we have the following additional equivalence classes:

1. q_e represented by the operator M_3 acting on a single edge e in R ,
2. p_e represented by the operator $M_4 = M_3M_2$ acting on a single edge e in R ,
3. q'_e represented by the product of M_3 acting on a single edge e in R and a long string operator ending in R and not overlapping with e (see Fig. 10(a)), and
4. p'_e represented by the product of M_4 acting on a single edge e in R and a long string operator ending in R and not overlapping with e (see Fig. 10(b)).

Note that both in Fig. 10(a) and Fig. 10(b), the electric charge excitation e can be freely moved without changing equivalence classes via appropriate (M_2) strings localized in R which do not intersect the edge where M_3 or M_4 acts.

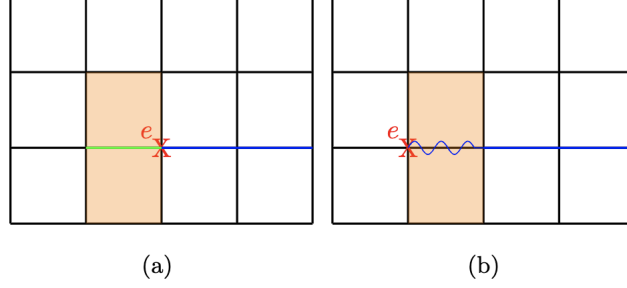


FIG. 10. (a) An example of the q'_e equivalence class where the long M_2 string (blue) doesn't intersect the edge e where M_3 acts (green). (b) An example of the p'_e equivalence class where the long M_2 string doesn't intersect the edge e where M_4 (wavy blue) acts. Note that M_4 anti-commutes with M_1 creating a pair of charges one of which fuses with the endpoint of the long M_2 string.

Using Eq. 28, we can obtain the following fusion rules involving m and the defects q_e and p_e .

$$\begin{aligned}
 q_e \otimes q_e &= p_e \otimes p_e = q'_e \otimes q'_e = p'_e \otimes p'_e = 0, \\
 q_e \otimes p_e &= p_e \otimes q_e = q_e \otimes p'_e = p'_e \otimes q_e = q'_e \otimes p_e = p_e \otimes q'_e = q'_e \otimes p'_e = p'_e \otimes q'_e = 0, \\
 q_e \otimes m &= m \otimes q_e = q_e, \\
 p_e \otimes m &= m \otimes p_e = p_e, \\
 q'_e \otimes m &= m \otimes q'_e = q'_e, \\
 p'_e \otimes m &= m \otimes p'_e = p'_e.
 \end{aligned} \tag{30}$$

The last four fusion rules above which show that a defect can absorb a m excitation imply the existence of magnetic monopoles outside any defect region as shown in Fig. 8 and discussed before. Note that the mobility of m excitations in the presence of defects¹⁰ is reflected in the fact that the last four fusion rules above hold for any edge e . We also note that we need to include the zero operator (equivalence class) for closure.

The fusion rules between e and the defects which can also be computed using Eq. 28 are more

¹⁰ The monopole actually can move through the defect region and becomes invisible (absorbed) only when it coincides with an edge of the defect region where M_3 acts.

complex, and are as listed below.

$$\begin{aligned}
q_e \otimes e &= q'_e \oplus p'_e, \\
e \otimes q_e &= q'_e \oplus 0, \\
q'_e \otimes e &= q_e, \\
e \otimes q'_e &= q_e \oplus 0, \\
p_e \otimes e &= p'_e \oplus q'_e, \\
e \otimes p_e &= p'_e \oplus 0, \\
p'_e \otimes e &= p_e, \\
e \otimes p'_e &= p_e \oplus 0.
\end{aligned} \tag{31}$$

These fusion rules are both non-commutative and non-Abelian.

The non-Abelian and non-commutative nature of the fusion rules can be explained as follows. Recall that the fusion product \otimes involves multiplying all possible elements of the two equivalence classes being fused. On the right hand side we write down all the equivalence classes that appear in such a product with a \oplus symbol indicating a logical 'or'. The non-commutative and non-Abelian nature of the fusion products $q_e \otimes e$ and $e \otimes q_e$ given above are illustrated in Fig. 11. As illustrated in this figure, we find that the non-Abelian properties of both these products arise from different choices of a representative long string operator e giving different results depending on whether the long string does or does not intersect the edge which supports the action of M_3 in the class q_e . The non-commutativity of both the fusion products as also illustrated in this figure follows from $M_2 M_3 = 0$ and $M_3 M_2 = M_4$. Similar computations can be used to understand the other non-Abelian and non-commutative fusion rules listed above.

The appearance of the 0 equivalence class on the right hand side illustrates that the e excitations have restricted mobility along certain paths in the presence of the defects as shown in Fig. 9 and discussed before.

The most striking non-commutative and non-Abelian elements of the fusion rules are actually those involving the identity sector (note that the toric code sector satisfies $e \otimes 1 = e = 1 \otimes e$,

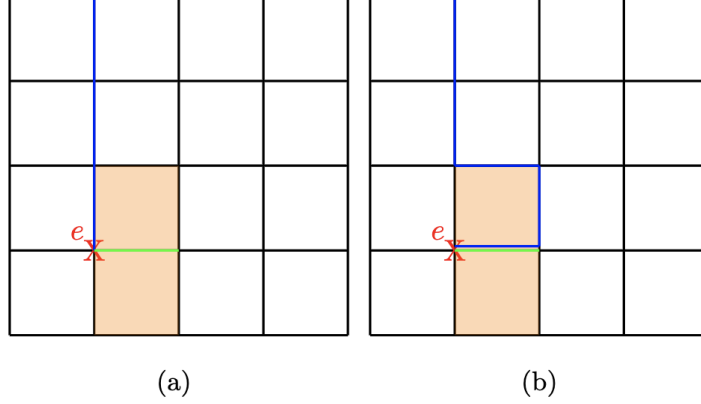


FIG. 11. Illustration of the fusion product $e \otimes q_e$ and $q_e \otimes e$ depending on the order of multiplication. (a) Shows one representative element of the e class multiplied with one of q_e creating q'_e . Also shows an element of q_e class multiplied with that of the e class creating q'_e . (See Fig. 10(a) for a representative of q'_e which is equivalent to the operator produced by these products.) (b) Shows another representative element of the e class that has an edge overlapping with the edge where M_3 acts. Since $M_2M_3 = 0$, the multiplication of this element with q_e produces 0. Since $M_3M_2 = M_4$, the multiplication of q_e with this element produces p'_e . (See Fig. 10(b) for a representative of p'_e which is equivalent to the operator produced by the latter product.)

$$m \otimes 1 = m = 1 \otimes m, \quad d \otimes 1 = d = 1 \otimes d):^{11}$$

$$\begin{aligned}
 1 \otimes q_e &= q_e \oplus 0, \\
 q_e \otimes 1 &= q_e \oplus p_e, \\
 1 \otimes q'_e &= q'_e \oplus 0, \\
 q'_e \otimes 1 &= q'_e \oplus p'_e, \\
 1 \otimes p_e &= p_e \oplus 0, \\
 p_e \otimes 1 &= p_e \oplus q_e, \\
 1 \otimes p'_e &= p'_e \oplus 0, \\
 p'_e \otimes 1 &= p'_e \oplus q'_e
 \end{aligned} \tag{32}$$

The above is a consequence of a contractible M_2 loop being equivalent to the identity operator as it is an element of the stabilizer monoid. Depending on whether this loop intersects the edge e or not, we get different results on the right hand side. The presence of non-invertible symmetries

¹¹ Since the left and right fusion products of q_e with 1 are different and can yield something different from q_e , etc., the symbol 1 standing for the equivalence class of the identity operator can be confusing. Nevertheless, it is easy to see that both left and right fusion product of any equivalence class with 1 yields back the equivalence class itself as one of the possibilities as in the standard multiplication with identity and $1 \otimes 1 = 1$.

gives rise to this striking feature that products with the identity sector is both non-Abelian and non-commutative. Physically this feature captures the ability of the M_2 contractible loop to detect the location of the defect as we have discussed before.

Furthermore, one can also check the above fusion rules are consistent with the associativity. Actually we can also determine $1 \otimes q_e$, $q_e \otimes 1$, etc. via associativity, and using $e \otimes e = 1$ and (31), since

$$1 \otimes q_e = e \otimes (e \otimes q_e) = e \otimes (q'_e \oplus 0) = q_e \oplus 0,$$

$$q_e \otimes 1 = (q_e \otimes e) \otimes e = (q'_e \otimes p'_e) \otimes e = q_e \oplus p_e,$$

etc. We can also check that the remaining fusion rules involving defects where only a single edge supports the action of M_3 or M_4 , along with those listed above, are associative, and all of these remaining ones can be determined via associativity as well, e.g. using $e \otimes m = m \otimes e = d$ and (31) we obtain

$$d \otimes q_e = e \otimes (m \otimes q_e) = m \otimes (e \otimes q_e) = q'_e \oplus 0,$$

etc.

The fusion of two defect excitations q_e and $q_{e'}$ corresponding to different edges e and e' creates a new equivalence class:

$$q_e \otimes q_{e'} = q_{ee'} \tag{33}$$

This proliferation of equivalence classes, i.e. scaling of the number of superselection sectors with the size of the system, is characteristic of fractonic models and captures the immobile nature of the corresponding fractonic excitations. However, we can readily see that some of the internal states of a larger defect configuration generated via actions of M_1 in the internal edges as discussed before, will not form a new equivalence class. For a larger defect configuration, the equivalence classes will denote inequivalent ways of producing the zero flux configurations solely via action of M_3 on the internal edges.

Finally, we note that in presence of larger defect configurations, one can have new equivalence classes, such as one involving even number of electric charges, due to the restricted mobility of electric charge excitations in the presence of the defects. For an illustration see Fig. 12 where a string of M_3 operators creates a wall of zero flux faces that partition the region R (shaded in gray) such that no string can pass from one half to the other without intersecting an edge where

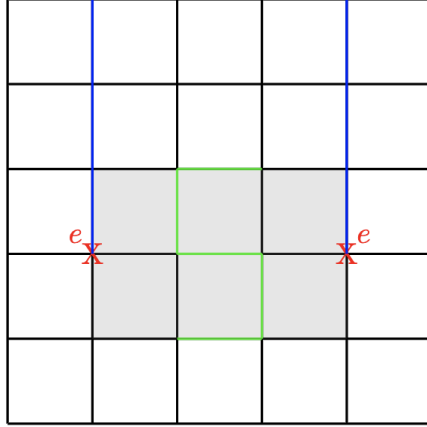


FIG. 12. Another nontrivial equivalence class. The gray shaded region including the edges on its boundary denotes the region of interest R . Note that the pair of electric charges cannot be converted to the ground state via the action of M_2 strings supported only within the region R . Any such M_2 string will have to intersect at least one green M_3 edge leading to the annihilation of the state.

M_3 acts. Therefore, adding a pair of long string operators creating an electric charge on each half afterwards creates a new equivalence class since these electric charges cannot be neutralized by a string operator located within R without acting on one of the edges where M_3 acts (the latter would annihilate the state as $M_2M_3 = 0$).

It is an interesting question to ask whether a subset of the fusion rules can be used to distinguish our model from other stabilizer code models supporting a qutrit on each edge and with non-invertible symmetries. We will discuss such models in the following concluding section. The quotienting of the equivalence classes by translation as done recently in [52] will be a complicated exercise but could be needed to distinguish between fractonic models of this type. We conclude this section by restating that the equivalence classes and their fusion rules do reflect the fundamental nature of the excitations in our model.

V. OUTRODUCTION

The model studied in this paper is part of a general class of stabilizer codes with a qutrit at each edge and with non-invertible symmetries. One such class is obtained from the family

$$M_1 \equiv \begin{pmatrix} r & 0 & 0 \\ 0 & 0 & 1 \\ 0 & 1 & 0 \end{pmatrix} = r \oplus X, \quad M_2 \equiv \begin{pmatrix} 0 & 0 & 0 \\ 0 & 1 & 0 \\ 0 & 0 & -1 \end{pmatrix} = 0 \oplus Z, \quad (34)$$

with r being a real number. (The case $r = -1$ corresponds to the present model.) We readily see that M_1 and M_2 anti-commute for arbitrary r . We can define the model in terms of elementary stabilizers, namely vertex operators A_v , each of which corresponds to a vertex v and is the product of M_1 acting on each edge converging at v , and plaquette operators B_f , each of which corresponds to a face f and is the product of M_2 acting on each edge bounding f . These elementary stabilizers commute with each other. The Hamiltonian is the sum of all the stabilizers up to an overall negative multiplicative constant.

It is easy to see that the toric code ground states, which are in the subspace obtained from the tensor product of the lower block two-dimensional subspaces of each edge, will be the ground states of these models unless r is a sufficiently large number. If r is sufficiently large, then the energy is minimized by the fully unentangled state

$$|G\rangle = \bigotimes_e \prod_e \begin{pmatrix} 1 \\ 0 \\ 0 \end{pmatrix}, \quad (35)$$

since in this case the vertex operator is more relevant at low energy and the lowest energy state should maximise the eigenvalues of each A_v . However, for intermediate values of r , energy minimization is a complex problem which would depend on the lattice.

Furthermore, one can check that M_3 (given by (20)) supported on any edge e and acting on the ground states generates fractonic confined defects (we obtain $M_1 M_3 = M_3 M_1 = -r M_3$, etc.). With $M_4 = M_3 M_2$ (given by (27)) we find that the only other different element in the products listed in (28) is

$$M_4 M_1 - r^{-1} M_1 M_4 = 0, \quad \text{while} \quad M_4 M_1 = M_4. \quad (36)$$

We postpone the analysis of such models and the construction of the fusion rules to a future publication.

Our model with $r = -1$, the model is actually self-dual (physically same as the dual model with M_1 and M_2 interchanged and living on the dual lattice) just like the toric code itself and this is reflected in the fusion rules discussed in the previous section, which are invariant under the exchange of e with m , q_e with p_e and q'_e with p'_e (see Eqs. (29), (30), (31) and (32)).

Generally, one can also consider different couplings for the vertex and plaquette operators. As for instance, by varying the ratio of these couplings in our model with two such couplings, we can obtain phases where the electric or magnetic charges are confined while going through the quantum critical topological point we have discussed in this work, as known to be the case in the toric code

sector [56, 57] (see also [58–61]). For the toric code, these phases can be captured by a \mathbb{Z}_2 gauge theory with confined/Higgsed phases included [34]. More recently, it has been shown that higher group gauge theories can describe phases of more general stabilizer codes [35–41].

A natural question therefore is whether one can construct a quantum field theory which reproduces the phase described by the model studied in this paper, and the other phases obtained by varying the couplings corresponding to the vertex and plaquette operators, by generalizing \mathbb{Z}_2 gauge theory. We expect that such a field theory should not only reproduce the ground states, expectation values of the loop operators and the dual loop operators and the fractonic defects with internal degrees of freedom which modify the behavior of deconfined excitations (allowing existence of magnetic monopoles and restricting mobility of electric charges) but also the fusion rules.

We readily realize that one can create an even larger family of such models featuring non-invertible symmetries and non-invertible defects with a qudit, i.e. a d level system at each edge of the lattice by choosing M_1 and M_2 (which would be $d \times d$ matrices) appropriately.¹² It is not obvious that the construction of the fusion category in this work readily generalizes to all such models with $d > 3$. Generally, the fusion product need not be associative. Furthermore, we need to also establish a connection between fusion rules and a notion of braiding (see [63] for related work). Finally, we would need to how renormalization group transformations can classify these models in terms of symmetries and fusion rules (see [52] for such a discussion in the context of fracton models).

It would be also interesting to see if one can construct a family of models where d can be varied and where we can take the limit $d \rightarrow \infty$. Analyzing this limit with an infinite-dimensional Hilbert space on every edge is similar to taking the large N limit in \mathbb{Z}_N gauge theory. We can expect that this limit can be described by a large N type quantum field theory.

We conclude with the observation that stabilizer codes have been useful in constructing models of holographic bulk reconstruction (see [64] for a recent review), and in this context fracton models (see [44] for an example) with non-invertible symmetries may give new insights into how gravity and spacetime can be reconstructed from degrees of freedom at the boundary.

ACKNOWLEDGMENTS

We thank Abhishek Chowdhury, Benoit Doucot, Debashis Ghoshal, Suresh Govindarajan, Prabha Mandayam, Giuseppe Policastro, P Ramadevi and Pratik Roy for many stimulating dis-

¹² See [62] for models with two qubits on each edge and a groupoid extension of the toric code. This model also features fractons.

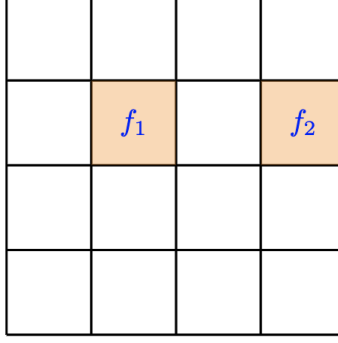


FIG. 13. The impossible two face excitation configuration on separated faces f_1 and f_2 .

cussions, and Arindam Lala, Archana Maji and Pratik Roy for initial collaboration in the early stages of this project. TK acknowledges support from the PMRF scheme of the Government of India. AM acknowledges support from IFCPAR/CEFIPRA funded project no 6304-3. AM and TK have been partly supported by the Center of Excellence initiative of the Ministry of Education of India, and AM has also been supported by the new faculty seed grant of IIT Madras.

Appendix A: Trace computations

1. Isolated defect faces are disallowed

Let us consider the following projector ($\mathcal{P}_2 = \mathcal{P}_{f_1, f_2}^d$)

$$\mathcal{P}_2 = (I - B_{f_1}^2) (I - B_{f_2}^2) \prod_v \frac{1}{2} (I + A_v) \prod_{f \neq f_{1,2}} \frac{1}{2} (B_f + B_f^2). \quad (\text{A1})$$

corresponding to states with the $f_{1,2}$ faces excited to the 0 eigenstate. We will assume that the faces $f_{1,2}$ do not share any edge as shown in Fig.13. This projector can be expanded as

$$\mathcal{P}_2 = \frac{1}{2^{|v|} 2^{|f|-2}} \left(I + \prod_v A_v \right) \left(\prod_f B_f^2 - \prod_{f \neq f_1} B_f^2 - \prod_{f \neq f_2} B_f^2 + \prod_{f \neq f_{1,2}} B_f^2 \right) + \text{traceless terms.} \quad (\text{A2})$$

Note that terms such as $(I - B_{f_1}^2) \prod_{f \neq f_1} B_f$ are traceless. Since $\prod_v A_v = I$ on a closed surface and

$$\prod_f B_f^2 = \prod_{f \neq \tilde{f}_1} B_f^2 = \prod_{f \neq \tilde{f}_2} B_f^2 = \prod_{f \neq \tilde{f}_{1,2}} B_f^2 = \prod_e M_e^2, \quad (\text{A3})$$

it is easy to see that

$$\text{Tr}(\mathcal{P}_2) = 0. \quad (\text{A4})$$

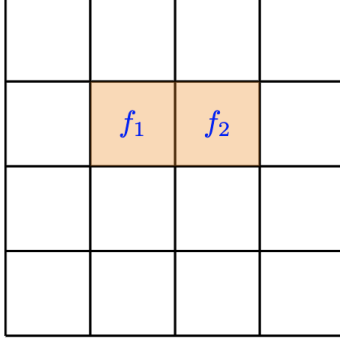


FIG. 14. A reproduction of a part of Fig. 4 from the main text showing two face excitations on connected faces $f_{1,2}$.

Thus states with two separated zero eigenvalue face excitations are disallowed. Similar computations can be used to show that any configuration with a disconnected face defect is disallowed.

2. Degeneracy of two zero flux face defects

The case when we have two connected face excitations $f_{1,2}$ is shown in Fig. 14. The projector in this case is ($\tilde{\mathcal{P}}_2 = \mathcal{P}_{f_1, f_2}^d$)

$$\tilde{\mathcal{P}}_2 = (I - B_{f_1}^2) (I - B_{f_2}^2) \prod_v \frac{1}{2} (I + A_v) \prod_{f \neq f_{1,2}} \frac{1}{2} (B_f + B_f^2), \quad (\text{A5})$$

which can be expanded as

$$\tilde{\mathcal{P}}_2 = \frac{1}{2^{|v|} 2^{|f|-2}} \left(I + \prod_v A_v \right) \left(\prod_f B_f^2 - \prod_{f \neq f_1} B_f^2 - \prod_{f \neq f_2} B_f^2 + \prod_{f \neq f_{1,2}} B_f^2 \right) + \text{traceless terms.} \quad (\text{A6})$$

Note that

$$\prod_f B_f^2 = \prod_{f \neq f_1} B_f^2 = \prod_{f \neq f_2} B_f^2 = \prod_e M_2^2, \quad (\text{A7})$$

however the last term $\prod_{f \neq f_{1,2}} B_f^2$ corresponds to M_2^2 acting on all edges except the edge shared by $f_{1,2}$, say $e_{1,2}$, where we have a 3×3 identity operator. Thus,

$$\prod_{f \neq f_{1,2}} B_f^2 = I_{e_{1,2}} \prod_{e \neq e_{1,2}} M_2^2. \quad (\text{A8})$$

We therefore obtain that

$$\text{Tr}(P_2) = \frac{2}{2^{|v|} 2^{|f|-2}} \left(2^{|e|} - 2^{|e|} - 2^{|e|} + 3 \times 2^{|e|-1} \right) = \frac{2^{|e|}}{2^{|v|} 2^{|f|-2}} = 2^{2g}. \quad (\text{A9})$$

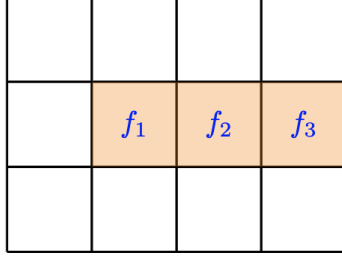


FIG. 15. A reproduction of Fig. 5 from the main text showing three faces $f_{1,2,3}$ are excited to the zero eigenstate.

3. Degeneracy of three zero flux face defects

The trace of the projector for a configuration with three connected defect faces as shown in Fig. 15 can be computed as follows. Let us label the edge connecting $f_{1,2}$ as e_1 and the edge connecting $f_{2,3}$ as e_2 . The projector onto this subspace is then ($\mathcal{P}_3 = \mathcal{P}_{f_1, f_2, f_3}^d$)

$$\mathcal{P}_3 = \prod_{i=1,2,3} (I - B_{f_i}^2) \prod_v \frac{1}{2} (I + A_v) \prod_{f \neq f_{1,2,3}} \frac{1}{2} (B_f + B_f^2), \quad (\text{A10})$$

which can be expanded as

$$\begin{aligned} \mathcal{P}_3 = & \left(- \prod_f B_f^2 + \prod_{f \neq f_1} B_f^2 + \prod_{f \neq f_2} B_f^2 + \prod_{f \neq f_3} B_f^2 - \prod_{f \neq f_{1,2}} B_f^2 - \prod_{f \neq f_{2,3}} B_f^2 - \prod_{f \neq f_{1,3}} B_f^2 + \prod_{f \neq f_{1,2,3}} B_f^2 \right) \\ & \times \frac{1}{2^{|v|} 2^{|f|-3}} \left(I + \prod_v A_v \right) + \text{traceless terms}. \quad (\text{A11}) \end{aligned}$$

$$\begin{aligned} \mathcal{P}_3 = & \left(- \prod_e M_2^2 + \prod_e M_2^2 + \prod_e M_2^2 + \prod_e M_2^2 - I_{e_1} \prod_{e \neq e_1} M_2^2 - I_{e_2} \prod_{e \neq e_2} M_2^2 - \prod_e M_2^2 + I_{e_1} I_{e_2} \prod_{e \neq e_{1,2}} M_2^2 \right) \\ & \times \frac{1}{2^{|v|} 2^{|f|-3}} \left(I + \prod_v A_v \right) + \text{traceless terms}, \quad (\text{A12}) \end{aligned}$$

where I denotes the 3×3 identity operator. Computing the trace of this projector we get

$$\text{Tr}(\mathcal{P}_3) = \frac{2}{2^{|v|} 2^{|f|-3}} \left(-2^{|e|} + 3 \times 2^{|e|} - 3 \times 2 \times 2^{|e|-1} - 2^{|e|} + 3^2 \times 2^{|e|-2} \right), \quad (\text{A13})$$

where we have carefully accounted for which of the internal edges $e_{1,2}$ have an identity and which have a M_2^2 . Simplifying the expression for the trace, we get

$$\text{Tr}(\mathcal{P}_3) = 2^{2g}. \quad (\text{A14})$$

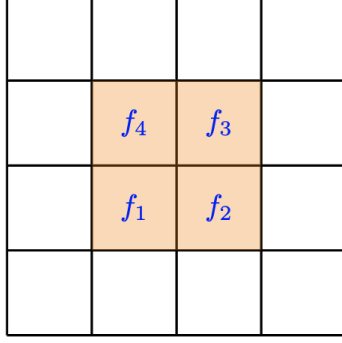


FIG. 16. A reproduction of Fig. 7 from the main text showing four faces $f_{1,2,3,4}$ are excited to the zero eigenstate. Note that we do not indicate the various internal states in this figure.

4. Degeneracy of four zero flux face defects

The trace of the projector onto the subspace with four defect faces arranged in a square, as shown in Fig.16, can be computed as follows. The projector onto this subspace is denoted by \mathcal{P}_4 and is given by ($\mathcal{P}_4 = \mathcal{P}_{f_1, f_2, f_3, f_4}^d$)

$$\mathcal{P}_4 = \prod_{i=1,2,3,4} (I - B_{f_i}^2) \prod_v \frac{1}{2} (I + A_v) \prod_{f \neq f_{1,2,3,4}} \frac{1}{2} (B_f + B_f^2), \quad (\text{A15})$$

expanding out the projector we get

$$\begin{aligned} \mathcal{P}_4 = & \left(\prod_f B_f^2 - \prod_{f \neq f_1} B_f^2 - \prod_{f \neq f_2} B_f^2 - \prod_{f \neq f_3} B_f^2 - \prod_{f \neq f_4} B_f^2 \right. \\ & + \prod_{f \neq f_{1,2}} B_f^2 + \prod_{f \neq f_{1,3}} B_f^2 + \prod_{f \neq f_{1,4}} B_f^2 + \prod_{f \neq f_{2,3}} B_f^2 + \prod_{f \neq f_{2,4}} B_f^2 + \prod_{f \neq f_{3,4}} B_f^2 \\ & \left. - \prod_{f \neq f_{1,2,3}} B_f^2 - \prod_{f \neq f_{1,2,4}} B_f^2 - \prod_{f \neq f_{1,3,4}} B_f^2 - \prod_{f \neq f_{2,3,4}} B_f^2 + \prod_{f \neq f_{1,2,3,4}} B_f^2 \right) \\ & \times \frac{1}{2^{|v|} 2^{|f|-4}} \left(I + \prod_v A_v + A_{v_0} + \prod_{v \neq v_0} A_v \right) + \text{traceless terms}. \quad (\text{A16}) \end{aligned}$$

Note that in this case we need to be careful to include the non-trivial contributions from the vertex operator on the vertex v_0 that is inside the defect region. Since the model is placed on a torus we have the constraints $\prod_v A_v = I$ and $\prod_{v \neq v_0} A_v = A_{v_0}$. The vertex operator A_{v_0} will contribute to the trace only if all the internal edges on which it acts have no M_2 or M_2^2 operator since $\text{Tr}(M_1 M_2) = \text{Tr}(M_1 M_2^2) = 0$. When evaluating the trace of the above expression one must

also recall that $\text{Tr}(A_{v_0}) = 1$. We can further simplify the projector as

$$\begin{aligned} \mathcal{P}_4 = & \left(\prod_f B_f^2 - \prod_{f \neq f_1} B_f^2 - \prod_{f \neq f_2} B_f^2 - \prod_{f \neq f_3} B_f^2 - \prod_{f \neq f_4} B_f^2 \right. \\ & + \prod_{f \neq f_{1,2}} B_f^2 + \prod_{f \neq f_{1,3}} B_f^2 + \prod_{f \neq f_{1,4}} B_f^2 + \prod_{f \neq f_{2,3}} B_f^2 + \prod_{f \neq f_{2,4}} B_f^2 + \prod_{f \neq f_{3,4}} B_f^2 \\ & \left. - \prod_{f \neq f_{1,2,3}} B_f^2 - \prod_{f \neq f_{1,2,4}} B_f^2 - \prod_{f \neq f_{1,3,4}} B_f^2 - \prod_{f \neq f_{2,3,4}} B_f^2 + \prod_{f \neq f_{1,2,3,4}} B_f^2 (I + A_{v_0}) \right) \\ & \times \frac{2}{2^{|v|} 2^{|f|-4}} + \text{traceless terms} . \quad (\text{A17}) \end{aligned}$$

Taking the trace of this expression we obtain

$$\text{Tr}(\mathcal{P}_4) = \frac{2}{2^{|v|} 2^{|f|-4}} \left(2^{|e|} - 4 \times 2^{|e|} + 4 \times 3 \times 2^{|e|-1} + 2 \times 2^{|e|} - 4 \times 3^2 \times 2^{|e|-2} + 3^4 \times 2^{|e|-4} + 2^{|e|-4} \right) \quad (\text{A18})$$

$$\text{Tr}(\mathcal{P}_4) = 9 \times 2^{2g}, \quad (\text{A19})$$

This 9 fold degeneracy can be accounted for in terms of operators as described in the main text.

-
- [1] Davide Gaiotto, Anton Kapustin, Nathan Seiberg, and Brian Willett, “Generalized Global Symmetries,” *JHEP* **02**, 172 (2015), arXiv:1412.5148 [hep-th].
 - [2] John McGreevy, “Generalized Symmetries in Condensed Matter,” (2022), 10.1146/annurev-conmatphys-040721-021029, arXiv:2204.03045 [cond-mat.str-el].
 - [3] Sakura Schafer-Nameki, “ICTP Lectures on (Non-)Invertible Generalized Symmetries,” (2023), arXiv:2305.18296 [hep-th].
 - [4] Shu-Heng Shao, “What’s Done Cannot Be Undone: TASI Lectures on Non-Invertible Symmetry,” (2023), arXiv:2308.00747 [hep-th].
 - [5] Yichul Choi, Ho Tat Lam, and Shu-Heng Shao, “Noninvertible Global Symmetries in the Standard Model,” *Phys. Rev. Lett.* **129**, 161601 (2022), arXiv:2205.05086 [hep-th].
 - [6] Pavel Putrov and Juven Wang, “Categorical Symmetry of the Standard Model from Gravitational Anomaly,” (2023), arXiv:2302.14862 [hep-th].
 - [7] Clay Cordova and Seth Koren, “Higher Flavor Symmetries in the Standard Model,” *Annalen Phys.* **535**, 2300031 (2023), arXiv:2212.13193 [hep-ph].
 - [8] Nathan Seiberg and Shu-Heng Shao, “Majorana chain and Ising model – (non-invertible) translations, anomalies, and emanant symmetries,” (2023), arXiv:2307.02534 [cond-mat.str-el].
 - [9] Rahul M. Nandkishore and Michael Hermele, “Fractons,” *Ann. Rev. Condensed Matter Phys.* **10**, 295–313 (2019), arXiv:1803.11196 [cond-mat.str-el].

- [10] Michael Pretko, Xie Chen, and Yizhi You, “Fracton Phases of Matter,” *Int. J. Mod. Phys. A* **35**, 2030003 (2020), arXiv:2001.01722 [cond-mat.str-el].
- [11] Cenke Xu, “Novel algebraic boson liquid phase with soft graviton excitations,” arXiv preprint cond-mat/0602443 (2006).
- [12] Cenke Xu and Petr Hořava, “Emergent gravity at a lifshitz point from a bose liquid on the lattice,” *Phys. Rev. D* **81**, 104033 (2010).
- [13] Michael Pretko, “Generalized electromagnetism of subdimensional particles: A spin liquid story,” *Phys. Rev. B* **96**, 035119 (2017).
- [14] Michael Pretko, “Subdimensional particle structure of higher rank $u(1)$ spin liquids,” *Phys. Rev. B* **95**, 115139 (2017).
- [15] Nathan Seiberg, “Field Theories With a Vector Global Symmetry,” *SciPost Phys.* **8**, 050 (2020), arXiv:1909.10544 [cond-mat.str-el].
- [16] Daniel Bulmash and Maissam Barkeshli, “Generalized $U(1)$ Gauge Field Theories and Fractal Dynamics,” (2018), arXiv:1806.01855 [cond-mat.str-el].
- [17] Han Ma, Michael Hermele, and Xie Chen, “Fracton topological order from the higgs and partial-confinement mechanisms of rank-two gauge theory,” *Phys. Rev. B* **98**, 035111 (2018).
- [18] Andrey Gromov, “Towards classification of fracton phases: The multipole algebra,” *Phys. Rev. X* **9**, 031035 (2019).
- [19] Nathan Seiberg and Shu-Heng Shao, “Exotic Symmetries, Duality, and Fractons in 2+1-Dimensional Quantum Field Theory,” *SciPost Phys.* **10**, 027 (2021), arXiv:2003.10466 [cond-mat.str-el].
- [20] Nathan Seiberg and Shu-Heng Shao, “Exotic \mathbb{Z}_N symmetries, duality, and fractons in 3+1-dimensional quantum field theory,” *SciPost Phys.* **10**, 003 (2021), arXiv:2004.06115 [cond-mat.str-el].
- [21] Nathan Seiberg and Shu-Heng Shao, “Exotic $U(1)$ Symmetries, Duality, and Fractons in 3+1-Dimensional Quantum Field Theory,” *SciPost Phys.* **9**, 046 (2020), arXiv:2004.00015 [cond-mat.str-el].
- [22] Michael Pretko and Leo Radzihovsky, “Fracton-elasticity duality,” *Phys. Rev. Lett.* **120**, 195301 (2018).
- [23] Andrey Gromov, “Chiral topological elasticity and fracton order,” *Phys. Rev. Lett.* **122**, 076403 (2019).
- [24] Wilbur Shirley, Kevin Slagle, Zhenghan Wang, and Xie Chen, “Fracton models on general three-dimensional manifolds,” *Phys. Rev. X* **8**, 031051 (2018).
- [25] Wilbur Shirley, Kevin Slagle, and Xie Chen, “Foliated fracton order from gauging subsystem symmetries,” *SciPost Phys.* **6**, 041 (2019).
- [26] Dominic J. Williamson, “Fractal symmetries: Ungauging the cubic code,” *Phys. Rev. B* **94**, 155128 (2016).
- [27] Trithep Devakul, Yizhi You, F. J. Burnell, and S. L. Sondhi, “Fractal Symmetric Phases of Matter,” *SciPost Phys.* **6**, 007 (2019).
- [28] Yizhi You, Trithep Devakul, F. J. Burnell, and S. L. Sondhi, “Subsystem symmetry protected topological order,” *Phys. Rev. B* **98**, 035112 (2018).

- [29] Dominic J. Williamson, Zhen Bi, and Meng Cheng, “Fractonic Matter in Symmetry-Enriched U(1) Gauge Theory,” *Phys. Rev. B* **100**, 125150 (2019), arXiv:1809.10275 [cond-mat.str-el].
- [30] A. Yu. Kitaev, “Fault tolerant quantum computation by anyons,” *Annals Phys.* **303**, 2–30 (2003), arXiv:quant-ph/9707021.
- [31] Daniel Gottesman, “Stabilizer codes and quantum error correction,” (1997), arXiv:quant-ph/9705052.
- [32] Jeongwan Haah, “Local stabilizer codes in three dimensions without string logical operators,” *Phys. Rev. A* **83**, 042330 (2011).
- [33] Sagar Vijay, Jeongwan Haah, and Liang Fu, “Fracton topological order, generalized lattice gauge theory, and duality,” *Phys. Rev. B* **94**, 235157 (2016).
- [34] Eduardo Fradkin and Stephen H. Shenker, “Phase diagrams of lattice gauge theories with higgs fields,” *Phys. Rev. D* **19**, 3682–3697 (1979).
- [35] John C Baez and Urs Schreiber, “Higher gauge theory,” arXiv preprint math/0511710 (2005).
- [36] Juan Pablo Ibieta-Jimenez, Marzia Petrucci, LN Xavier, and Paulo Teotonio-Sobrinho, “Topological entanglement entropy in d-dimensions for abelian higher gauge theories,” *Journal of High Energy Physics* **2020**, 1–44 (2020).
- [37] R Costa de Almeida, JP Ibieta-Jimenez, J Lorca Espiro, and P Teotonio-Sobrinho, “Topological order from a cohomological and higher gauge theory perspective,” arXiv preprint arXiv:1711.04186 (2017).
- [38] Alex Bullivant, Marcos Calçada, Zoltán Kádár, Paul Martin, and Joao Faria Martins, “Topological phases from higher gauge symmetry in 3+ 1 dimensions,” *Physical Review B* **95**, 155118 (2017).
- [39] Alex Bullivant, Marcos Calçada, Zoltán Kádár, Joao Faria Martins, and Paul Martin, “Higher lattices, discrete two-dimensional holonomy and topological phases in (3+ 1) d with higher gauge symmetry,” *Reviews in Mathematical Physics* **32**, 2050011 (2020).
- [40] Maissam Barkeshli, Yu-An Chen, Po-Shen Hsin, and Ryohei Kobayashi, “Higher-group symmetry in finite gauge theory and stabilizer codes,” (2022), arXiv:2211.11764 [cond-mat.str-el].
- [41] Salvatore D. Pace and Xiao-Gang Wen, “Emergent higher-symmetry protected topological orders in the confined phase of U(1) gauge theory,” *Phys. Rev. B* **107**, 075112 (2023), arXiv:2207.03544 [cond-mat.str-el].
- [42] Chetan Nayak, Steven H Simon, Ady Stern, Michael Freedman, and Sankar Das Sarma, “Non-abelian anyons and topological quantum computation,” *Reviews of Modern Physics* **80**, 1083 (2008).
- [43] Jurgen Fuchs, “Fusion rules in conformal field theory,” *Fortsch. Phys.* **42**, 1–48 (1994), arXiv:hep-th/9306162.
- [44] Han Yan, “Hyperbolic fracton model, subsystem symmetry, and holography,” *Phys. Rev. B* **99**, 155126 (2019), arXiv:1807.05942 [hep-th].
- [45] Claudio Chamon, “Quantum glassiness in strongly correlated clean systems: An example of topological overprotection,” *Phys. Rev. Lett.* **94**, 040402 (2005).
- [46] Sergey Bravyi, Bernhard Leemhuis, and Barbara M Terhal, “Topological order in an exactly solvable 3d spin model,” *Annals of Physics* **326**, 839–866 (2011).

- [47] Sagar Vijay, Jeongwan Haah, and Liang Fu, “A new kind of topological quantum order: A dimensional hierarchy of quasiparticles built from stationary excitations,” *Phys. Rev. B* **92**, 235136 (2015).
- [48] Beni Yoshida, “Exotic topological order in fractal spin liquids,” *Phys. Rev. B* **88**, 125122 (2013).
- [49] Miguel Jorge Bernabé Ferreira, Pramod Padmanabhan, and Paulo Teotonio-Sobrinho, “2d quantum double models from a 3d perspective,” *Journal of Physics A: Mathematical and Theoretical* **47**, 375204 (2014).
- [50] Shriya Pai and Michael Pretko, “Fractons from confinement in one dimension,” *Phys. Rev. Res.* **2**, 013094 (2020), arXiv:1909.12306 [cond-mat.str-el].
- [51] Miguel Jorge Bernabé Ferreira, Juan Pablo Ibieta Jimenez, Pramod Padmanabhan, and Paulo Teôtonio Sobrinho, “A recipe for constructing frustration-free hamiltonians with gauge and matter fields in one and two dimensions,” *Journal of Physics A: Mathematical and Theoretical* **48**, 485206 (2015).
- [52] Shriya Pai and Michael Hermele, “Fracton fusion and statistics,” *Phys. Rev. B* **100**, 195136 (2019), arXiv:1903.11625 [cond-mat.str-el].
- [53] Jeongwan Haah, “Commuting pauli hamiltonians as maps between free modules,” *Communications in Mathematical Physics* **324**, 351–399 (2013).
- [54] Jeongwan Haah, “Algebraic methods for quantum codes on lattices,” *Revista colombiana de matematicas* **50**, 299–349 (2016).
- [55] David Tong, “Lectures on the Quantum Hall Effect,” (2016) arXiv:1606.06687 [hep-th].
- [56] Franz J. Wegner, “Duality in generalized ising models and phase transitions without local order parameters,” *J. Math. Phys.* **12** (1971), 10.1063/1.1665530.
- [57] John B. Kogut, “An introduction to lattice gauge theory and spin systems,” *Rev. Mod. Phys.* **51**, 659–713 (1979).
- [58] N. Read and Subir Sachdev, “Large-n expansion for frustrated quantum antiferromagnets,” *Phys. Rev. Lett.* **66**, 1773–1776 (1991).
- [59] X. G. Wen, “Mean-field theory of spin-liquid states with finite energy gap and topological orders,” *Phys. Rev. B* **44**, 2664–2672 (1991).
- [60] F. Alexander Bais, Peter van Driel, and Mark de Wild Propitius, “Quantum symmetries in discrete gauge theories,” *Phys. Lett. B* **280**, 63–70 (1992), arXiv:hep-th/9203046.
- [61] Juan Martin Maldacena, Gregory W. Moore, and Nathan Seiberg, “D-brane charges in five-brane backgrounds,” *JHEP* **10**, 005 (2001), arXiv:hep-th/0108152.
- [62] Pramod Padmanabhan and Indrajit Jana, “Groupoid Toric Codes,” (2022), arXiv:2212.01021 [quant-ph].
- [63] Wilbur Shirley, Kevin Slagle, and Xie Chen, “Fractional excitations in foliated fracton phases,” *Annals Phys.* **410**, 167922 (2019), arXiv:1806.08625 [cond-mat.str-el].
- [64] Tanay Kibe, Prabha Mandayam, and Ayan Mukhopadhyay, “Holographic spacetime, black holes and quantum error correcting codes: a review,” *Eur. Phys. J. C* **82**, 463 (2022), arXiv:2110.14669 [hep-th].